

# Non-identical anyon algebras from compact-field quantum geometry

O. Kashuba<sup>1</sup>, Ram Mummadavarapu<sup>1\*</sup> and R.-P. Riwar<sup>1</sup>

<sup>1</sup> Peter Grünberg Institute, Theoretical Nanoelectronics, Forschungszentrum Jülich, D-52425 Jülich, Germany

\* [r.mummadavarapu@fz-juelich.de](mailto:r.mummadavarapu@fz-juelich.de)

## Abstract

Compact scalar field theories on lattices are capable of describing a large class of many-body systems, such as interacting bosons, superconducting circuit networks, spin systems and more. We show that a generic quantum geometric many-body coupling induces quantized Chern couplings, implementing a lattice network version of a Florianini-Jackiw theory. Quantum geometry thus unlocks a direct mapping from scalar fields to anyons with fractional exchange phases, relevant for quantum error correction codes and quantum chemistry computation applications. In contrast to more familiar local Chern-Simons constructions with a uniform level, the compact-phase quantum geometry considered here yields pair-dependent topological couplings that can be nonlocal in node space and are encoded by a nonuniform first-Chern matrix. This feature introduces the notion of non-identical anyons, i.e., excitations that do not mutually satisfy the same exchange statistics. Such non-identical exchange statistics open up a microscopic pathway to a virtually unexplored class of non-local field theories breaking the Wigner superselection rule, allowing to explore non-local communication (all-to-all qubit gates) with local control.

## 1 Introduction

One of the central pursuits in condensed matter physics is to realize and control anyonic excitations with fractional exchange statistics (e.g., the fractional quantum Hall effect [1, 2] or spin liquids [3]), as they are expected to provide a basis for topological quantum field theories and quantum computing. There has furthermore been significant effort to simulate such strongly correlated phenomena on lattices or meta-materials, which traditionally involved engineering specific Hamiltonians in real-space lattices. This often involves utilising exotic materials [4] or large, complex architectures to mimic the target field theory [5, 6], leading to significant scalability challenges [7].

To our knowledge, all topological materials studied so far exhibit a *single* type of anyon. For instance, a fractional quantum Hall bar (e.g., at filling fraction  $1/K$ ) hosts an anyon  $\eta(x)$ , with exchange statistics  $\eta(x)\eta(y) = e^{i2\pi/K}\eta(y)\eta(x)$  for all positions  $x, y$ . Composite systems (such as tunneling between two quantum Hall bars with different filling fractions) can, in principle allow for two types of anyons to interact, but fundamental principles such as charge quantization and the Wigner superselection rule limit the types of allowed interactions.

Based on a generic quantum geometric treatment of many-body interactions, we here show that any scalar boson maps onto an anyonic theory of the form

$$\eta_z \eta_{z'} = e^{i2\pi q_{zz'}/p} \eta_{z'} \eta_z \quad (1)$$

where  $z$  is the lattice index,  $p$  is an integer, and  $q$  is an integer-valued matrix of essentially *arbitrary* shape (subject only to the antisymmetry constraint,  $q^T = -q$ ). Conventional identical

anyons have  $q_{zz'} = q$ , i.e., the exchange statistics are the same for all  $z > z'$  (and  $-q$  for  $z < z'$ ). For instance,  $q = 1$  and  $p = 2$  yield a regular fermionic lattice. As soon as  $q$  depends nontrivially on the lattice index, we obtain a generic network of *non-identical* anyons.

Interpreting the scalar boson as a plasmonic field carrying charges, anyons are commonly associated with charge fractionalisation (e.g., in the fractional quantum Hall effect). Crucially, in our setup, charge quantization is built in from the get-go, and the resulting anyons carry fractional *flux* rather than fractional charge. As a consequence, charge-conserving processes permit generic interaction terms of the form  $\eta_z^m \eta_{z'}^{m'}$ , substantially enlarging the class of allowed anyon couplings compared with more familiar constructions. Moreover, upon including a trivial node  $z_0$ , for which  $\eta_{z_0} = \mathbf{1}_{z_0}$ , the effective low-energy Hamiltonian can contain terms of the form  $\mathbf{1}_{z_0} \eta_z + \text{h.c.}$ , corresponding to an unpaired anyon and thereby breaking the Wigner superselection rule (valid in the here considered non-relativistic limit). This creates the possibility of nonlocal communication protocols with local control, linking the present construction both to quantum hardware applications and to broader foundational questions about locality and superselection in quantum mechanics [8–10], specifically to how local realism and Wigner superselection for fermionic systems [11, 12] may be formulated on an axiomatic level. Our work is motivated by a new paradigm [13–15] that recently emerged in the context of quantum circuits, designed to overcome scaling limitations of quantum hardware. Instead of defining topological properties in real space, they can be defined in the abstract space spanned by the compact scalar fields  $\phi_z$  (e.g., superconducting phases  $\Delta e^{i\phi}$ , or relatedly, bosonic phases  $b^{(\dagger)} \sim e^{\pm i\phi}$ ). In this context, non-reciprocal gyrator elements have recently gained significant traction [13, 16]. They have been proposed [15] to realize an effective magnetic field on a 2D lattice in  $\phi$ -space, realizing the Hofstadter butterfly spectrum at non-integer gyration conductance.

The compactness of the field  $\phi$  plays a pivotal role. For superconducting circuits, this compactness represents charge quantization, whose importance has been widely studied [17–19]<sup>1</sup>. A compact  $\phi$  space provides a natural analogue to the Brillouin zone, forming a higher dimensional torus  $\mathbb{T}^Z$ . Any gapped eigenspectrum on that Brillouin zone has associated with it a Berry curvature, whose integral yields a quantized Chern number. For multi-terminal Josephson junctions, this generic feature has been predicted to allow for the creation of topological matter in virtually *any* dimension [14] without necessarily involving exotic materials, simply by adding a sufficiently large number of circuit nodes. This mechanism has been explored in various contexts, including Andreev bound states [14, 21, 22], tunnel junctions [23–25], and quantum dots [26, 27], as well as generalizations to higher-order invariants [28], and has spurred considerable progress on the experimental side in the control and measurement of multiterminal Josephson junctions [29–32]. Recently, there have emerged some early efforts to explore the impact of the Berry curvature on qubit architectures [33–35]. Here, we show that the inherent many-body quantum geometry of these systems supplies the mechanism for anyon formation and fractionalization. We demonstrate in particular that the low-energy physics of any many-body multi-node system must map onto a set of generic (non-identical) anyons carrying integer charge and fractional flux, see Fig. 1. We thus provide blueprints for quantum hardware to simulate highly general interacting fermionic or anyonic systems, which are of both applied and fundamental interest, and (as already stated) go beyond conventional, Wigner parity-conserving field theories.

Our work relies on mapping the circuit dynamics onto a particle on a high-dimensional torus, where the geometric Berry curvature yields Landau levels and an algebra of anyons determined by Chern numbers (gyrators), which are quantized as per Dirac’s magnetic monopole argument [36]. The additional presence of regular (non-topological) couplings (in the circuit

<sup>1</sup>Whether or not the superconducting phase  $\phi$  is compact (or more precisely, closed) depends on the existence of a mechanism to entangle with the number turns a given system performs in  $\phi$ -space; see Refs. [18–20].

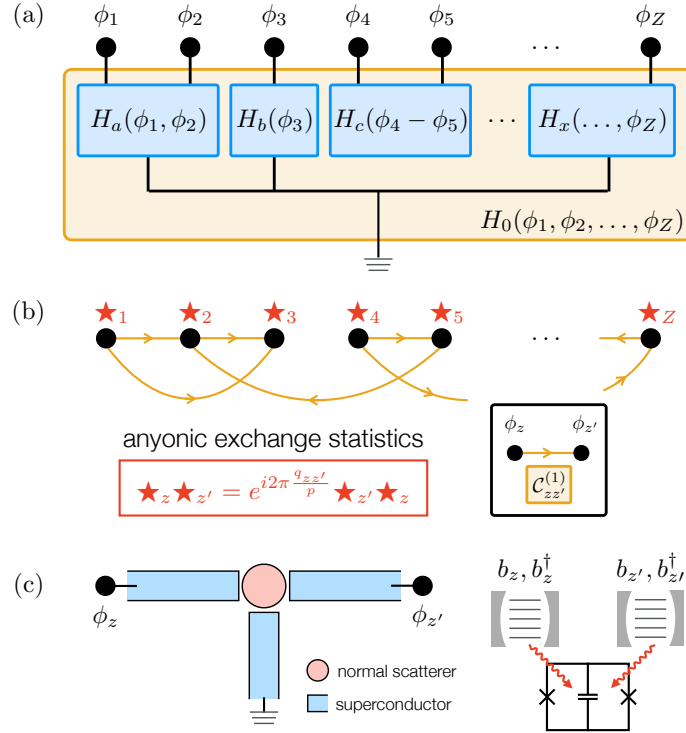


Figure 1: Main result of our work. (a) We consider a lattice with nodes  $z$  described by compact fields  $\phi_z$ , where generic couplings are mediated by extra degrees of freedom described by Hamiltonians  $H_{a,b,\dots}$  summarized into a total multi-terminal Hamiltonian  $H_0$ . (b) By including many-body quantum fluctuations, the quantum geometric contribution of  $H_0$  maps the lattice onto a network of circuit nodes coupled by gyrators with quantized gyration conductance given by a (first) Chern number. This results in anyonic excitations, one for each node, with rational fractional exchange statistics depending on the gyration conductance matrix. (c) Possible realizations of coupler systems between two nodes with nonzero Chern number, either with superconducting circuits (left) or quantum cavities (right).

language, regular Josephson effects) lifts the ground state degeneracy, allowing for the anyons to tunnel and interact. For the case of two circuit nodes, we show that anyon tunneling manifests as a hybrid effect between Aharonov-Bohm and Aharonov-Casher phases and a fractional dual Josephson effect, effectively revealing flux fractionalization [37].

Overall, both charge and flux control in combination with a tunable Josephson effect form a set of quantum gates for anyonic excitations. This framework enables the simulation of Majorana fermions for quantum chemistry [38], solid state systems [39, 40], and the Sachdev-Ye-Kitaev model [41, 42] through local control. Unlike standard qubit architectures requiring non-local Jordan-Wigner strings [43], our platform features naturally emerging exchange statistics and local addressability, facilitating error correction codes like GKP [44], potentially mitigating scalability issues [45, 46].

This approach also allows us to explore field theories breaking the fermion parity superselection rule [47] and establishes a minimal scalar gauge theory distinct from standard vector Chern-Simons formulations [48]. In the outlook, we provide some ideas for establishing even deeper connections between non-reciprocal interactions in quantum circuits and the fractional quantum Hall effect.

## 2 Preface: compact scalar fields

To set the stage, we consider a network of  $Z$  lattice points (from now on called nodes). To each node  $z$  ( $z = 1, \dots, Z$ ), we assign a field  $\phi_z$ , which we refer to as a phase. Quantum theories for such a field can be generically expressed via a Lagrangian,  $L(\{\dot{\phi}_z, \phi_z\})$ , depending on all phases and their phase velocities. The Hamiltonian is obtained from the Lagrangian by the usual Legendre transformation within ordinary canonical quantization,  $H = \sum_z n_z \dot{\phi}_z - L$ , where the canonical momentum  $n_z = \partial_{\dot{\phi}_z} L$  satisfies the regular commutation relation  $[\phi_z, n_{z'}] = i\delta_{zz'}$ .

Let  $\phi_z$  be compact (on a ring of size  $2\pi$ ). The total Hilbert space thus corresponds to a  $Z$ -dimensional torus, and the overall wave function  $\psi(\{\phi_z\})$  must be single-valued on that torus. Such scalar compact field theories describe a considerable number of systems. For superconducting quantum circuit networks,  $\phi_z$  corresponds to the superconducting phase, and  $n_z$  is the Cooper pair number on a given node. A bosonic system (e.g., quantum optics) with ladder operators  $b_z^\dagger$  can likewise be expressed with such fields, most conveniently in the limit of dense bosons [49], where the ladder operators are approximated as  $b_z^\dagger \sim e^{i\phi_z}$  ( $b_z \sim e^{-i\phi_z}$ ) and the boson number is  $b_z^\dagger b_z \sim n_z$ . Relatedly, chiral Luttinger liquids describing quantum Hall edge states are known to be compact scalar fields [50]. Furthermore, mappings are known to the XXZ model [51], and to the XY model, which in turn maps to the Coulomb gas via the Villain transformation, as well as to the discrete Gaussian model describing solid-on-solid physics [52], just to name a few more. Overall, it can be noted that for many of the above cases,  $\phi_z$  describes a collective *many-body* degree of freedom.

The Lagrangian typically has the following generic form,

$$L_0 = \sum_{zz'} \dot{\phi}_z C_{zz'} \dot{\phi}_{z'} - \epsilon_0(\{\phi_z\}), \quad (2)$$

where the kinetic term proportional to the phase velocities provides quantum fluctuations of  $\phi_z$  (once the theory is quantized). Compactness of the phase here can be guaranteed by imposing that the potential energy  $\epsilon_0$  be single-valued on the  $Z$ -dimensional torus – or in other words,  $2\pi$ -periodic in all  $\phi_z$ .

The central physics that we focus on here comes in the form of an *additional* nonreciprocal term,  $L = L_0 + L_G$ ,

$$L_G = - \sum_z \dot{\phi}_z A_z, \quad (3)$$

where the vector-potential  $A_z$  is likewise a function of all phases. One might naively expect that  $A_z$  likewise needs to be single-valued on the torus, but in actuality, the theory allows for topological terms linear in  $\phi_z$ , related to the well-known Dirac monopole quantization argument for quantum mechanics on closed manifolds (see further below for an in-depth discussion).

Such topological terms are well-known in the context of chiral edge states describing fractional quantum Hall physics. Take the ordinary Chern-Simons Lagrangian in 2+1 dimensions (for pedagogical reviews, see [48, 50]),

$$L_{CS} = \frac{k}{4\pi} \iint_{\Sigma} dx dy \epsilon^{\mu\nu\lambda} a_\mu \partial_\nu a_\lambda, \quad (4)$$

where  $x, y$  are coordinates of the (here continuous) spatial dimensions, and the level  $k$  must be integer quantized (and the indices  $\mu = 0, 1, 2$  stand for time and the two space components). One can isolate the edge state (at the boundary  $\partial\Sigma$  of the 2D volume  $\Sigma$ ) simply by gauge fixing  $a_0 = 0$  and further restricting the theory to  $a_1 = \partial_x \phi$  and  $a_2 = \partial_y \phi$  (using Stokes' theorem),

$$L_{\text{edge}} = \frac{k}{4\pi} \int_{\partial\Sigma} dl \cdot (\dot{\phi} \nabla \phi). \quad (5)$$

The resulting action is known as the Floreanini-Jackiw action, providing a field theoretic access to anyonisation of fermions ( $k$  odd) and bosons ( $k$  even), mapping to the Laughlin state with fractional filling (at  $k > 1$ ).

However, all known treatments of such Chern-Simons-type interactions share the following features: (i) they emerge from top-down field theoretic considerations, and are not derived directly from microscopic principles, (ii) the Chern-Simons level  $k$  is homogeneous in space, such that the entire system is described by one type of anyon, and (iii) the coupling is local, as evidenced by the fact that only the first spatial derivative ( $\sim \nabla\phi$ ) enters. Motivated by recent progress within the superconducting circuit community (where the emergence and functioning of non-reciprocal terms similar to those in  $L_g$  has been discussed in various contexts [13, 15, 33, 34]) we provide in what follows a platform-independent microscopic derivation of topological non-reciprocal interactions via many-body quantum geometry, thus closing the gap of issue (i) for lattice systems (when position space  $x, y$  is discrete, and not limited to two spatial dimensions). By doing so we gain access to an entirely unexplored class of quantum field theories with surprising nonlocal properties, vastly exceeding the limitations of (ii) and (iii).

### 3 Nonreciprocity from quantum geometry

Our starting point is the generic lattice introduced above, with nodes  $\phi_z$ . While (as emphasized already) this lattice may describe a wide range of physical systems, for the sake of concreteness we use circuit language in what follows and refer to  $\phi_z$  as a phase and to the canonically conjugate  $n_z$  as a charge. It is furthermore useful to introduce a reference point for the phases, i.e., all values of  $\phi_z$  are to be taken with respect to a phase ground set to zero. Changing this reference point corresponds to a global  $U(1)$  shift. Invariance under that shift represents charge conservation. In circuit language, this reference point is the actual electrical ground.

We now include a generic coupling between all  $Z$  nodes, and (optionally) to ground. While different nodes are in general coupled with different physical connections, we can cast all of these details into a single, all-encompassing “black box” circuit element. Under a concise set of assumptions, we will show that the black box generically reduces to a network of pairwise connections each described by a (first) Chern number. While we here (for the sake of generality) consider a generic multiterminal setup where we impose no upper bound on the number of nodes  $Z$ , we will show in a moment that any arbitrarily large network can always be decomposed into elementary building blocks with an individual nonzero Chern number between two active nodes, see, e.g., circuit diagrams like in Fig. 1.

We emphasize that the internal degrees of freedom of the black box element are *additional*, intrinsic physical degrees of freedom beyond the scalar field. For superconducting circuits, we think of the black box as a multiterminal Josephson junction (or a network thereof) connecting different islands. In the quantum optics context, we can think of it as a coupler device between cavities. We describe the black box by a Hamiltonian as a function of the phases,  $H_0(\{\phi_z\})$ . The only further restrictions we place on this system are that it has a nondegenerate ground state with a finite gap to the first excited state, and the above compactness condition, i.e., the Hamiltonian shall be  $2\pi$ -periodic in all phases  $\phi_z$ , indicating integer quantization of  $n_z$ . Finally, the emergence of nonzero Chern numbers will imply time-reversal symmetry breaking.

We now include a kinetic coupling. For circuits, this corresponds to capacitive couplings between circuit nodes to ground and between each other. For quantum optics, the same mechanism accounts for self- and cross-Kerr terms of the cavities. This yields the Hamiltonian

$$H = 2e^2 \sum_{zz'} n_z (C^{-1})_{zz'} n_{z'} + H_0(\{\phi_z\}). \quad (6)$$

Expressing the black box Hamiltonian in terms of its eigenstates  $H_0 = \sum_k \epsilon_k |k\rangle\langle k|$  (the  $\phi_z$ -

dependence of energy  $\epsilon_k$  and state  $|k\rangle$  is no longer explicitly denoted), and fixing the index of the nondegenerate ground state as  $k = 0$ , we perform a geometric version of a Born-Oppenheimer approximation, which was first developed in the context of atomic physics by Mead and Truhlar [53] (and whose importance was recently appreciated for Josephson junctions [33, 34]), where projecting onto  $|0\rangle$  yields the low-energy description,

$$H \approx 2e^2 \sum_{zz'} (n_z + A_z)(C^{-1})_{zz'}(n_{z'} + A_{z'}) + \epsilon_0, \quad (7)$$

with the Berry connections  $A_z = i\langle 0|\partial_{\phi_z}|0\rangle$ . In addition to the canonical charge  $n_z$ , there is the kinetic charge  $n_z + A_z$ , whose commutator (between nodes  $z$  and  $z'$ ) is gauge-invariant,

$$[n_z + A_z, n_{z'} + A_{z'}] = i(\partial_{\phi_{z'}}A_z - \partial_{\phi_z}A_{z'}) = i\mathcal{B}_{zz'}, \quad (8)$$

and given by the Berry curvature  $\mathcal{B}_{zz'}$ . Note that the kinetic charge is the physical charge on the nodes. For circuits, it determines the electric field between nodes.

We thus arrive via a well-defined low-energy approximation on the Hamiltonian level at the very same vector potential term given in the Lagrangian term of Eq. (3). Adding charge energy terms and the potential energy  $\epsilon_0$ ,  $L = \frac{1}{8e^2} \sum_{zz'} \dot{\phi}_z C_{zz'} \dot{\phi}_{z'} + L_G - \epsilon_0$ , and following standard quantization rules, we can directly connect the Lagrangian with the Hamiltonian of Eq. (7).

Contrary to a vast majority of work being done in the solid state context, where the Berry curvature is usually defined in the single-particle eigenspectrum (of, e.g., electrons moving within the solid), the above is a *many-body* quantum geometric effect – by virtue of the coupling to the many-body field  $\phi_z$ . As such, the energy bands of  $H_0$  have no meaningful notion of an occupation number in the second quantized language: the state  $|0\rangle$  represents directly a many-body ground state.

## 4 Gyration conductance quantization

Specifically in the quantum circuit context, it was recently noted [33, 35] that geometric effects in the multiterminal Josephson effect are deeply related to quantum circuit versions of gyrator elements [13, 15], see Fig. 2. In particular, the gyrator in Refs. [13, 15] is described by a simple vector potential, which is linear in  $\phi_z$ . Generalized to an arbitrary number of nodes, it reads

$$A_z = \sum_{z'} g_{zz'} \phi_{z'}, \quad (9)$$

where the matrix  $g$ , called gyration conductance matrix, can in principle take arbitrary real values. Note that  $g$  is not gauge invariant. Crucially, though, depending on whether or not we impose compactness of the superconducting phases  $\phi_z$ , there are further constraints on  $g$ , rooted in gauge properties on compact spaces. These form the basis of our endeavour.

To begin, note that if we assume  $\phi_z$  compact (more precisely, closed—default assumption throughout this work), the first Chern number, defined as

$$C_{zz'}^{(1)} = \frac{1}{2\pi} \int_0^{2\pi} d\phi_z \int_0^{2\pi} d\phi_{z'} \mathcal{B}_{zz'}, \quad (10)$$

is integer quantized. As indicated in the introduction, nontrivial geometric (Berry curvature) effects, including a resulting nonzero Chern number, have been predicted to emerge for *conventional* multiterminal Josephson junctions [14, 23–27, 54] with broken time-reversal symmetry.

Devices as simple as a three-terminal Josephson junction with a central normal metal scattering region, see Fig. 1c (left panel), can host a nontrivial Chern number [14], provided the central scattering region breaks time-reversal symmetry (threading the central region with a magnetic field) [22].

With our above emphasis on the platform independence, we note that the engineering of similar Hamiltonians as in Refs. [14, 23–27, 54] can also be realized in other systems, e.g., in cavities where the superconducting phase operators  $e^{\pm i\phi_z}$  in  $H_0$  are replaced with boson ladder operators  $b_z^{(\dagger)}$  changing the photon number. For concreteness, in Appendix A, we present an example of a two-cavity Hamiltonian implementing a Chern insulator, defined in the 2D lattice spanned by the number of photons in the respective cavities, see also the right panel in Fig. 1c.

In general, all Berry curvatures  $\mathcal{B}_{zz'}$ , and the potential energy  $\epsilon_0$  depend on  $\phi_z$  in a periodic (and thus nonlinear) fashion. This means that diagonalizing the low-energy Hamiltonian in Eq. (7) is still a hard problem. However, we can explicitly separate the topological transition in the form of a non-zero Chern number from any other  $\phi_z$ -dependent terms, thus “peeling off” the topological component of the theory from the otherwise non-linear, strongly correlated physics. To this end, we define  $\mathcal{B}_{zz'} = \mathcal{C}_{zz'}^{(1)}/2\pi + \delta\mathcal{B}_{zz'}$  where the integral of  $\delta\mathcal{B}_{zz'}$  over  $\phi_z, \phi_{z'}$  is zero per definition. This procedure can be reflected by a similar separation of the vector potential into  $A_z = a_z + \delta A_z$ , where  $a_z$  needs to be chosen, such that it returns the nonzero Chern number part when plugged into Eq. (8). Consequently,  $a_z$  must be linear, and can be written by means of the gyration conductance, see Eq. (9), i.e.,  $a_z = \sum_{z'} g_{zz'} \phi_{z'}$  with the constraint on the conductance matrix,

$$(g - g^T)_{zz'} = \frac{\mathcal{C}_{zz'}^{(1)}}{2\pi}. \quad (11)$$

The remaining  $\delta A_z$  can always be chosen to be periodic in all phases  $\phi_z$ . The total Hamiltonian can thus be separated into linear and nonlinear parts,

$$H = H_{\text{linear}} + H_J, \quad (12)$$

where the linear part reads

$$H_{\text{linear}} = 2e^2 \sum_{zz'} (n_z + a_z)(C^{-1})_{zz'}(n_{z'} + a_{z'}). \quad (13)$$

All nonlinear terms, either due to  $\delta A_z$  or  $\epsilon_0$ , are cast into the remaining term  $H_J$ , which (as we discuss in more detail below) physically represents a generic Josephson effect between nodes. The linear term can be diagonalized exactly. The resulting eigenmodes and emergent excitations of  $H_{\text{linear}}$  remain useful to describe the physics even for finite  $H_J$  as long as  $H_J$  remains sufficiently small. This is the regime we focus on in what follows: we will show that  $H_{\text{linear}}$  gives rise to bosonic energy eigenstates (generalized Landau levels), where each Landau level has a finitely degenerate subspace. This subspace is composed of anyons. When including a finite  $H_J$ , the degeneracy lifts, and the anyons start to couple, giving rise to a myriad of effects that can either be mapped onto known systems, or give rise to surprising non-local effects that have not been studied previously.

Before that, an important aside: one may object that the linear term  $a_z$  seems to fundamentally break  $2\pi$ -periodicity and, thus, compactness in  $\phi_z$ , such that it appears impossible to find a meaningful gauge for the vector potential on the torus. This problem can however be mended by invoking a curvature  $\tilde{\mathcal{B}}_{zz'}$  distinct from the Berry curvature by subtracting  $\mathcal{C}_{zz'}^{(1)}$  Dirac-delta-like “horns” [55],

$$\tilde{\mathcal{B}}_{zz'} = \mathcal{B}_{zz'} - 2\pi \sum_i \mathcal{K}_{zz'}^{(i)} \delta(\phi_z - \phi_z^{(i)}) \delta(\phi_{z'} - \phi_{z'}^{(i)}), \quad (14)$$

at arbitrary positions  $\phi_{z^{(i)}}$  of the integer heights  $\mathcal{K}_{zz'}^{(i)}$ , such that  $\sum_i \mathcal{K}_{zz'}^{(i)} = \mathcal{C}_{zz'}^{(1)}$ . This curvature satisfies by construction the Gauss-Bonnet theorem (note that the boundary term is absent due to the manifold being closed)

$$\frac{1}{2\pi} \int_0^{2\pi} d\phi_z \int_0^{2\pi} d\phi_{z'} \tilde{\mathcal{B}}_{zz'} = \chi_T = 0 \quad (15)$$

where the Euler characteristic  $\chi_T$  of the torus is zero. It further allows for a gauge choice of  $a_z$  (and thus of  $A_z$ ), such that its curl yields  $\tilde{\mathcal{B}}$  instead of  $\mathcal{B}$ . This vector potential is locally given by Eq. (9) but globally contains jumps to satisfy  $2\pi$  periodicity in the superconducting phases. This construction is helpful for explicit numeric calculations by, e.g., discretizing  $\phi_z$ -space (in the Appendix B, we explicitly consider a 2-dimensional system for illustration). At any rate, note that for quantum coherent trajectories on the torus, the above introduced horns do not change the dynamics, simply because the phase picked up when circumventing them is  $e^{i2\pi} = 1$ . Therefore, while  $\tilde{\mathcal{B}}$  is necessary for a consistent construction of the low-energy  $H$  in  $\phi$ -space, we can nonetheless work with  $\mathcal{B}$  in other basis representations, as long as we take care that the construction of the pertinent operator algebra respects phase compactness.

Overall,  $H_{\text{linear}}$  maps to a particle moving in a constant magnetic field on a  $Z$ -dimensional torus. Importantly, we stress that the word ‘‘particle’’ has to be interpreted with care: as already emphasized, the theory was already formulated in a second-quantized language. The ‘‘positions’’ ( $\phi_z$ ) and ‘‘momenta’’ ( $n_z$ ) of this particle are already by definition many-body operators. For instance, there exists no physically meaningful way to generalize above torus-analogy to the case of having many particles on a torus. That being said, the image of a particle is nonetheless helpful, as it becomes obvious that the well-known Dirac quantization condition for magnetic monopoles [36] is perfectly equivalent to the integer quantization of the Chern numbers. We further note that since each Chern number is defined in a 2D subspace, the magnetic field can always be decomposed into components connecting two nodes  $z$  and  $z'$ . It is in this sense, that we can always think of the generic  $(Z + 1)$ -terminal junction ( $Z$  nodes plus ground) as a network of simpler fundamental elements connecting two out of the  $Z$  nodes, as announced above.

The above discussion is in significant contrast to many existing works on gyrators [13, 15, 56–58] where the gyration conductance matrix  $g - g^T$ , can take on any real value (which may have different physical realizations). Crucially, for the enticing proposition to realize Hofstadter butterfly physics on emergent lattices in  $\phi$ -space [15] the non-integer nature of the effective magnetic field is very much a *prerequisite*: if  $g - g^T$  were quantized as in Eq. (11) above, the circuit behaviour in Ref. [15] would be trivial and equivalent to the gyrators being absent altogether. Relatedly, Ref. [15] could only provide a consistent quantum mechanical treatment when assuming extended  $\phi$ 's (by adding additional linear inductive shunts). As outlined above, with the here present quantum geometric origin of the nonreciprocal interaction, the constraint on  $g$  given in Eq. (11) is fundamentally linked to compact  $\phi_z$ . However, there are other regimes where nonreciprocity occurs within a finite frequency window [13] or requires periodic driving [58]. To our knowledge, there is no consensus yet as to possible constraints on  $g$  beyond the assumptions stated in this work. At any rate, as we elaborate in what follows, an integer-valued  $g - g^T$  is (in contrast to the considerations in Ref. [15]) far from having a trivial effect in the above setups—to the contrary, they give rise anyonic excitations, providing the opportunity to explore a plethora of nontrivial emergent phenomena.

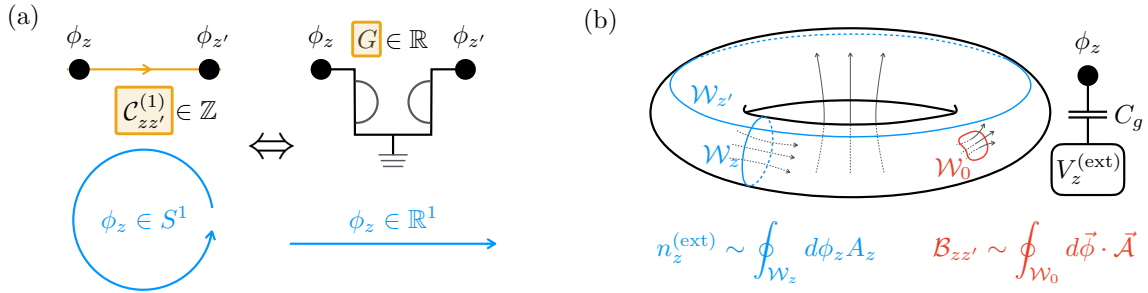


Figure 2: Important aspects regarding phase compactness. (a) A nonzero Chern number between two nodes (left) essentially maps onto a gyrator (right, denoted by Tellegen’s symbol), however, with the difference that the Chern number (equivalent to the gyration conductance) must be integer quantized when defined on compact superconducting phases. Conceptually, the circuit element is a three-terminal device (one terminal to ground), where in the left symbol, we omit the explicit representation of the ground for simplicity. (b) Upon including capacitive coupling, the dynamics of a circuit with  $Z$  nodes reduces to a fictitious particle moving in a magnetic field on a  $Z$ -dimensional torus (here shown for two dimensions). Contrary to the ordinary Landau level problem in extended space, the gauge invariance on the torus comes with a number of complications. For instance, in addition to the trivial  $\mathcal{W}_0$  loops there are two types of nontrivial loops  $\mathcal{W}_z$  and  $\mathcal{W}_{z'}$ , which cannot be controlled by the value of the magnetic field only. The phase accumulated across these extra loops is defined by gate-voltage induced offset charges.

## 5 Landau levels on higher dimensional torus

We here diagonalize the Hamiltonian  $H_{\text{linear}}$ . It will be convenient to define the kinetic charge  $N_z = n_z + a_z$  (which differs from the previously introduced kinetic charge by including only the topological part of the vector potential  $a_z$ , and not the full  $A_z$ ). If  $\phi_z$  were extended,  $H_{\text{linear}}$  would be readily solved through a standard Bogoliubov transformation and yield (infinitely degenerate) Landau levels in a  $Z$ -dimensional system. Let us briefly recapitulate the diagonalization for extended  $\phi_z$ , before we delve into the compact case. In this case of the extended  $\phi_z$ , the kinetic charges  $N_z$  can be expressed as linear combinations terms of bosonic ladder operators  $a_j^{(\dagger)}$  switching the Landau level number, resulting in the diagonal form,  $H = \sum_j \omega_j a_j^\dagger a_j$  (the index  $j$  indicates that in more than 2 dimensions, Landau levels have in general many cyclotron eigenfrequencies). At the same time, the Landau-level degeneracy can be captured by zero modes (a set of operators commuting with  $N_z$ , and thus with  $H$ ), which can be regarded as a kinetic flux,

$$\Phi_z = \phi_z - \sum_{z'} \left( \frac{1}{g - g^T} \right)_{zz'} N_{z'}. \quad (16)$$

This construction of course necessitates that  $\det(g - g^T) \neq 0$ , in order for  $g - g^T$  to be invertible. Furthermore, since  $g - g^T$  is skew-symmetric (essentially by definition), the inverse can only exist if  $Z$  is even. Both even  $Z$  and  $\det(g - g^T) \neq 0$  will be the default assumption in the remainder of this work. We will in a moment relate invertibility to the existence of higher Chern numbers. The non-invertible case will be touched upon at the end of this work.

Phase compactness has an important impact on the Fock space of our system: the Landau levels have a finite degeneracy. This feature has explicitly been shown for the two-dimensional torus [55, 59] – a result we here generalize to arbitrary dimensions. To see this, we note that

while the construction of the bosonic  $N_z$  is still valid on a torus<sup>2</sup>, we have to construct a set of kinetic phase operators that satisfy  $2\pi$ -periodicity, which is accomplished with exponentiation,  $e^{i\Phi_z}$ . These operators still satisfy  $[e^{i\Phi_z}, N_z] = 0$ , and provide the algebra

$$e^{im\Phi_z} e^{im'\Phi_{z'}} = e^{i2\pi mm' q_{zz'}/p} e^{im'\Phi_{z'}} e^{im\Phi_z}, \quad (17)$$

where  $m^{(\prime)} \in \mathbb{Z}$ . The variables  $\{\phi_z\}$  live on a closed and compact manifold, from which it follows that the variables  $\{\Phi_z\}$  are compact too. We therefore find that for compact  $\phi_z$ , the excitations within a given Landau level give rise to an *abelian anyonic exchange statistics*, with the exchange phase matrix

$$\frac{q_{zz'}}{p} = \frac{1}{2\pi} \left( \frac{1}{g - g^T} \right)_{zz'}. \quad (18)$$

As the second equality indicates, the exchange phase is always a rational number with  $q$  being an integer-valued matrix, and  $p$  an integer scalar. As a matter of fact,  $p$  is equal to the  $Z/2$  Chern number (we remind that  $Z$  is even, and  $\epsilon$  is the Levi-Civita symbol),

$$p = C^{(Z/2)} = \sum_{z_1, \dots, z_Z} \frac{\epsilon^{z_1, \dots, z_Z} C_{z_1 z_2}^{(1)} \dots C_{z_{Z-1} z_Z}^{(1)}}{2^{Z/2} (Z/2)!}, \quad (19)$$

whereas the matrix  $q$  is given as a ‘‘transposed’’  $Z/2 - 1$  Chern number

$$q_{zz'} = \overline{C}_{zz'}^{(Z/2-1)} = \sum_{z_3, \dots, z_Z} \frac{\epsilon^{z', z, z_3, \dots, z_Z} C_{z_3 z_4}^{(1)} \dots C_{z_{Z-1} z_Z}^{(1)}}{2^{Z/2-1} (Z/2 - 1)!}. \quad (20)$$

Translating this to the language of skew-symmetric matrices,  $p$  is the Pfaffian of the matrix  $C^{(1)} = 2\pi(g - g^T)$ . The matrix  $q$  plays the same role for inversion of skew-symmetric matrices, as the adjoint one for general matrices. The ordinary adjoint matrix consists of minors which are determinants of the smaller matrices  $A^{\hat{z}\hat{z}'}$  obtained by removing one row  $z$  and one column  $z'$  from matrix  $A$  [60]. In our case, the determinants are substituted by Pfaffians, where the two columns and rows  $z$  and  $z'$  are removed symmetrically from the original matrix. Consequently, the inverse matrix is matrix  $q$  divided over the Pfaffian of the original skew-symmetric matrix. The Pfaffian can be calculated by the recursive formula [61]

$$\text{Pf} C = \sum_{zz'=1}^{2n} (-1)^{z+z'+1+\theta(z-z')} c_{zz'} \text{Pf} C^{\hat{z}\hat{z}'}, \quad (21)$$

from which one can immediately see, that  $p$  and any element of  $q$  are also integer.

To provide specific examples, for two nodes ( $Z = 2$ ) we simply have (in matrix representation)

$$\frac{q}{p} = \frac{1}{C^{(1)}} \begin{pmatrix} 0 & -1 \\ 1 & 0 \end{pmatrix}, \quad (22)$$

where there is only one first Chern number, hence the omission of node indices. In contrast, for four nodes ( $Z = 4$ ), we find

$$\frac{q}{p} = \frac{1}{C^{(2)}} \begin{pmatrix} 0 & -C_{34}^{(1)} & C_{24}^{(1)} & -C_{23}^{(1)} \\ C_{34}^{(1)} & 0 & -C_{14}^{(1)} & C_{13}^{(1)} \\ -C_{24}^{(1)} & C_{14}^{(1)} & 0 & -C_{12}^{(1)} \\ C_{23}^{(1)} & -C_{13}^{(1)} & C_{12}^{(1)} & 0 \end{pmatrix}, \quad (23)$$

<sup>2</sup>Energy levels on a periodic but extended system and a compact system are related by a Bloch theorem. Therefore, the Landau levels must persist in exactly the same form for both choices.

where the second Chern number emerges in the denominator,  $C^{(2)} = C_{12}^{(1)}C_{34}^{(1)} - C_{13}^{(1)}C_{24}^{(1)} + C_{14}^{(1)}C_{23}^{(1)}$ . This calculation can be continued in analogy for higher  $Z$ .

We draw from the above the following conclusions. The requirement  $q, p \in \mathbb{Z}$  follows simply from the first Chern numbers  $C_{zz'}^{(1)}$  being all integer. The existence of the inverse of  $g - g^T$  requires  $C^{(Z/2)}$  (the highest possible Chern number for a device with  $Z$  nodes) to be nonzero. Note though, that this by no means implies that  $\det(g - g^T) = 0$  gives rise to any problematic behaviour whatsoever; in that case one simply has to carefully separate zero and nonzero eigenvalues of  $g - g^T$  and construct the kinetic flux operators accordingly, again see the end of this work.

Overall, the above result illustrates that in spite of the system being in principle fully described by the first Chern numbers connecting two nodes, the resulting (nonzero) second and higher Chern numbers appear very prominently in the anyonic exchange statistics of multi-node devices. As a matter of fact, all Chern numbers also appear in the energy spectrum. Specifically for  $Z = 2, 4$ , we calculate the Landau level frequencies for the case of dominant capacitive coupling ground (for simplicity we assume the capacitance matrix to be  $C_{zz'} = C_g \delta_{zz'}$ , such that the model only includes a capacitance to ground). For  $Z = 2$ , we obtain a single cyclotron mode,  $H = \omega a^\dagger a$ , with frequency

$$\omega = \frac{2e^2}{\pi C_g} C^{(1)}, \quad (24)$$

whereas for  $Z = 4$ , there are two modes,  $H = \omega_+ a_+^\dagger a_+ + \omega_- a_-^\dagger a_-$ , with frequencies

$$\omega_\pm = \frac{2e^2}{\sqrt{8}\pi C_g} \sqrt{|q|^2 \pm \sqrt{|q|^4 - 4[C^{(2)}]^2}} \quad (25)$$

where we defined the norm for  $q$ ,  $|q|^2 = \sum_z \sum_{z' > z} [q_{zz'}]^2$ . As a consequence, both second and first Chern numbers can be directly tracked in an experiment measuring the circuits resonance frequencies (such as, e.g., a standard dispersive readout). Let us return to the anyonic subspace within a Landau level. Given that the anyonic exchange phase is rational, we can infer that an appropriate group representation of the operators  $e^{i\Phi_z}$  must be cyclic and discrete, since  $e^{ip\Phi_z}$  is guaranteed to commute with everything, and thus must return an ordinary c-number (consistent with one of the fundamental properties of a parafermionic anyon). For generic cases, we refer to the pertinent literature for recipes to construct group representations for operators satisfying Eq. (17). The way to the solution of this problem paved by finite groups theory starts from finding the factor group. One can build the regular representation and exploit Cauchy–Frobenius lemma [62–64] to identify the group structure. One can decompose the group in such a way into point groups, the irreducible representations of which are known. At any rate, for the special cases we consider in the remainder of this work it is easy to find explicit representations, where each Landau level is exactly  $p$ -fold degenerate. The simplest case that can be computed exactly is that of two nodes, mapping onto the 2D torus, where  $p = (C)^{(1)}$ . In the regular Landau problem (on an extended 2D space), the level degeneracy is given by the ratio of the sample area divided by the size of the corresponding cyclotron orbit. On the torus, essentially the same logic remains true, leading to a  $p = (C)^{(1)}$  fold degeneracy, see also Fig. 6 in Appendix B.

We emphasize that this degeneracy can be (and in general will be) lifted, as soon as the anyons experience a finite coupling due to nonzero  $H_J$ , a physical feature that will be discussed in the now following sections. We stress though, that lifting the degeneracy does not mean a breaking of the topological phase. As long as there are nonzero Chern numbers in the circuit (expressed by the matrix  $C_{zz'}$ ), the abelian anyons satisfying the resulting exchange relationship Eq. (17) remain the system's fundamental excitations. This type of protection is

ensured by Weyl points within the intrinsic degrees of freedom of the multiterminal junctions, Eq. (6), which cannot be annihilated by small deformations. For example, in [14], Weyl point separation depends on a superconducting phase controlled by a loop flux. A main source for Chern number fluctuations is quasiparticle poisoning, but given long quasiparticle lifetimes (seconds to minutes), this is a minor concern. Overall, anyon coupling and the ensuing degeneracy lifting are thus not detrimental effects (as long as they are weak enough, and do not lead to Landau level mixing), but instead provide an interesting finite anyon dynamics and enable the observation of nontrivial anyonic physics, and anyon manipulation relevant for quantum information applications. Specifically, for quantum information processing, it is in general desirable for the anyon couplings to be tunable, and thus invariably subject to noise (a feature that is in fact true for any quantum computation proposal, whether the fundamental excitations forming the qubit are of topological nature or not). Such noise sources have to be counteracted by dedicated quantum error correction codes. The specific advantage of our proposal lies in the fact that anyons emerge already with very low node numbers and by using only conventional materials, reducing certain aspects of the hardware requirements. Moreover, Chern numbers are in general tunable [14], which allows for an in-situ control of the anyonic exchange statistics, relevant for a flexible quantum simulation hardware.

## 6 Uncommon gauge properties: integer charges and fractional fluxes

The emergence of anyonic excitations always comes hand in hand with the fractionalization of some physical quantity. We will show in the following, that when sticking to the quantum circuit interpretation of the field  $\phi_z$ , the here emerging anyons carry fractional *flux* while (contrary to the fractional quantum Hall effect) charge stays integer, and that both flux fractionalization and exchange statistics can be probed by a finite  $H_J$ . This endeavour will bring to light surprising gauge properties which seem at the surface to imply the breaking of gauge invariance altogether – an issue that can be resolved because the Chern-Simons physics emerges from concrete microscopic (quantum geometric) considerations.

Concerning the nonzero  $H_J$ , note that both  $\epsilon_0$  and  $\delta A_z$  are  $2\pi$ -periodic in  $\phi_z$ , and can therefore be expressed in terms of a generic Fourier series of harmonics, i.e.,

$$\epsilon_0 = \sum_{m_1, m_2, \dots, m_z} \epsilon_{m_1, m_2, \dots, m_z} e^{im_1 \phi_1} e^{im_2 \phi_2} \dots e^{im_z \phi_z} \quad (26)$$

with  $m_z \in \mathbb{Z}$  (and similarly for  $\delta A_z$ ). If this Josephson effect is weak compared to the cyclotron frequency, we can project onto the lowest Landau level with the operator  $P_0$  (such that  $a_j P_0 = P_0 a_j = 0$  for all cyclotron modes  $j$ , while the anyon subspace stays untouched). For the first harmonic, we get

$$P_0 e^{i\phi_z} P_0 = \alpha e^{i\Phi_z}, \quad (27)$$

where the scalar prefactor is real, smaller than 1, and equal to  $\alpha = \text{tr}[e^{\sum_z' (\frac{1}{g-g^T})_{zz'} N_{z'}} P_0]$ . It simply arises from projecting out the Landau level excitations, which renormalizes the amplitude of the Josephson effect. The same principle generalizes for arbitrary higher harmonics,

$$P_0 e^{i \sum_z m_z \phi_z} P_0 \sim e^{i \sum_z m_z \Phi_z}. \quad (28)$$

Note that we also get the same qualitative result for terms due to  $\delta A_z$ , which in lowest order provide extra terms of the form  $P_0 N_{z'} e^{i \sum_z m_z \phi_z} P_0 \sim e^{i \sum_z m_z \Phi_z}$ . The only difference here is that the renormalization prefactor changes shape due to the extra  $N_z$  operator.

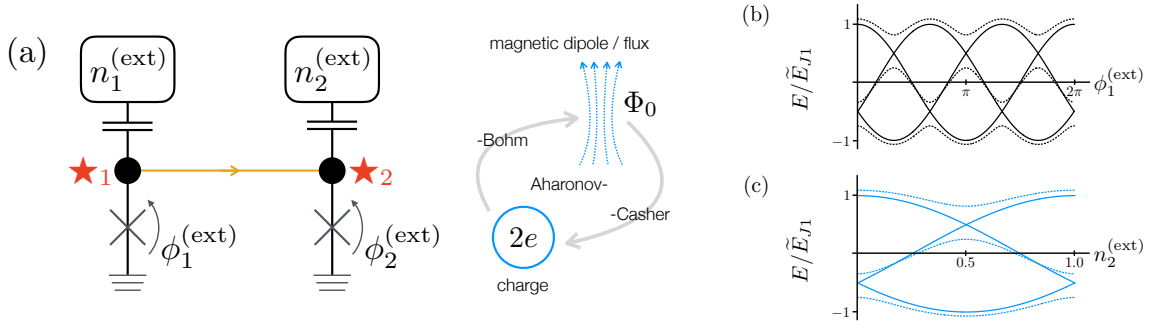


Figure 3: Gapping the degeneracy of the lowest Landau level by means of Josephson couplings reveals the intricate gauge properties on the torus, and the resulting nonlocal interplay between charge and flux. (a) Minimal example of a circuit with two nodes, connected by a Chern number, each additionally coupled to ground via a Josephson junction. Coupling to an external magnetic field is represented by flux shifts for each Josephson junction,  $\phi_{1,2}^{(\text{ext})}$ , and interaction to a static electric field is accounted for by a capacitive coupling to a gate voltage, resulting in the offset charges  $n_{1,2}^{(\text{ext})}$ . The external fields result in a finite flux and charge dispersion, which can be interpreted as a superposition of an Aharonov-Bohm, respectively, Aharonov-Casher effect. Panels (b) and (c) show the different periodicity with respect to applied flux at node 1 and applied offset charge at node 2, here for  $p = C^{(1)} = 3$ . The broken periodicity with respect to the offset charge indicates that the anyons carry a fractional flux (but integer charge). The solid lines show the case when only one site is shunted by a Josephson junction (i.e.  $\tilde{E}_{J2} = 0$ ), while the dashed lines mark the case when  $\tilde{E}_{J2} = \frac{1}{2}\tilde{E}_{J1}$ .

Overall, a finite  $H_J$  lifts the degeneracy of the Landau level. For an explicit example, let us add a regular Josephson effect between ground and node  $z$ ,  $-E_J \cos(\phi_z)$ . Projected to the lowest Landau level, this yields the Hamiltonian  $H = -\tilde{E}_J \cos(\Phi_z)$ , revealing a fine structure of the degenerate subspace. The Josephson energy is renormalized,  $E_J \rightarrow \alpha E_J \equiv \tilde{E}_J$  in accordance with Eq. (27). For example, for  $Z = 2$  the prefactor is simply  $\alpha = e^{-\pi/(2p)}$  (i.e., the higher the value of the first Chern number  $C^{(1)}$ , the weaker the renormalization). A Josephson effect between two nodes  $\sim \cos(\phi_z - \phi_{z'})$  is treated on the exact same footing, yielding at low energies a tunneling of anyons between sites  $z$  and  $z'$ ,  $\sim \cos(\Phi_z - \Phi_{z'})$ . This corresponds to a tunneling of anyons between different nodes.

Importantly, the resulting energy splitting is affected by the coupling of external electromagnetic fields, which, in the circuit context are known as Aharonov-Bohm *and* Aharonov-Casher effects [19, 37, 65–68]. The inclusion of both applied voltages (Aharonov-Casher) and magnetic fluxes (Aharonov-Bohm) requires some attention to detail. The latter is in principle straightforwardly included as a classical flux offset,  $\phi_z \rightarrow \phi_z + \phi_z^{(\text{ext})}$ , which arises from a coupling to an external magnetic field [69]. However, the question is, whether this shift in  $\phi_z$  has to be applied to all parts in the Lagrangian, whenever  $\phi_z$  appears, only to selected terms (e.g., we could shift all  $\phi_z$  by an offset within  $\epsilon_0$ , while gyration terms  $\sim \phi_z \dot{\phi}_{z'}$  are unchanged). The answer is that it depends on the physical realization of the circuit. In the following, we will apply the shift only to Josephson effects, and justify this choice after the fact.

The Aharonov-Casher effect emerges when including an offset charge to node  $z$ ,  $n_z \rightarrow n_z + n_z^{(\text{ext})}$ , by applying the gate voltage  $V_{gz}$  to node  $z$ , such that  $n_z^{(\text{ext})} = C_{gz} V_{gz} / (2e)$ , where  $C_{gz}$  is the capacitance between node  $z$  and the gate attached to it. It is well known that for circuits with compact phases (such as the charge qubit [37]), the energy spectrum is sensitive to charge offsets—giving rise to the so-called charge dispersion effect (which was,

e.g., recently used to track quasiparticle poisoning [70, 71] or to probe higher Josephson harmonics [72], indicating that offset charge noise is slow enough to allow reliable measurements). For external voltage sources, such offsets can be added readily in the capacitive term of the original microscopic Hamiltonian, Eq. (6), which is then simply carried over to the low energy theory, Eq. (7). Note however, that the quantum geometric component may have its own contribution. In quantum mechanical terms, quantum systems on compact manifolds pick up a phase as the coordinate travels along the periodic  $\phi_z$  and completes one cycle. For a two-dimensional subspace  $(\phi_z, \phi_{z'})$ , this means that the system is not fully determined by the Berry curvature  $\mathcal{B}_{zz'}$  alone, since it only determines the geometric phases of paths that do not probe the torus topology (i.e., paths that can be shrunk to single points). The torus however offers two more distinct types of paths (see Fig. 2) whose phases need to be fixed, thus nominally contributing to  $n_z^{(\text{ext})}$ .

At this stage, we can already see that there is a peculiar interconnectedness between charge and flux offsets: the Chern number part of the vector potential depends on  $\phi_z$ , see Eq. (9), such that offset charges can be swallowed by offset fluxes and vice versa. Let us focus on pure external voltage sources [see also Fig. 3(a)], and adding phase offsets as discussed previously. Then, the respective flux and charge offsets carry over to the kinetic quantities  $N_z$  and  $\Phi_z$  respectively. When projecting to the lowest Landau level, the Josephson effect thus reveals both types of shifts as

$$H = -\tilde{E}_J \cos \left( \underbrace{\Phi_z + \phi_z^{(\text{ext})} - 2\pi \sum_{z'} \frac{q_{zz'}}{p} n_{z'}^{(\text{ext})}}_{\Phi_z^{(\text{ext})}} \right), \quad (29)$$

where we defined the total phase shift  $\Phi_z^{(\text{ext})}$  as the sum of flux and charge offsets. Since the eigenvalues of  $e^{i\Phi_z}$  are discrete and bounded, neither flux nor charge offsets can be gauged away (unless they take on precise quantized values). Instead, in the low-energy projection, the circuit's eigenspectrum is explicitly sensitive to both the Aharonov-Bohm phase (regular Josephson effect) and the Aharonov-Casher phase (effectively a dual Josephson effect), with the latter being *fractional*, as it directly reflects the anyonic exchange statistics. This is in contrast to the regular fractional Josephson effect, where the periodicity in the Aharonov-Bohm phase is altered, (e.g., the  $4\pi$ -periodic dependence of Majorana-based junctions on the Aharonov-Bohm phase).

This demonstrates that the anyonic excitations carry a *superposition* of integer charge and fractional flux. This duality can be better understood if we perceive the flux as a magnetic dipole [65], where we cannot distinguish whether the charge is moving around the flux, or vice versa. We can detect only a mutual movement or charge and flux with respect to each other [as illustrated in Fig. 3(a)]. Overall, the duality between charge and phase manifests itself in Eq. (29) as a highly nonlocal interdependency between applying a flux offset between ground and node  $z$  and adding a gate (inducing an offset charge) at another node  $z'$  defined by the connectivity of the gyrator network. The nonlocality of charge and flux gate operations stems from the elimination of the propagation of electro-magnetic waves (valid under the assumption that the speed of light is much faster than any of the other time scales, typical for circuit QED considerations [69]). The non-locality of the theory (in the non-relativistic regime) will reemerge as an important ingredient further below. As a side remark, note that since the Josephson effect is tunable, its fluctuations can cause energy resonance lines to broaden. This broadening can be expected to be small: in a dc-SQUID, the critical current is typically tuned by flux modulations on the order of one flux quantum, whereas flux noise usually scales between  $10^{-5}$  to  $10^{-7}$  flux quanta [73].

Let us illustrate both the fractionalization and interdependency of charge and phase explicitly for  $Z = 2$ . The exchange statistics in Eq. (22) are here represented, e.g., by the con-

structions

$$e^{i\Phi_1} = Z_p \quad e^{i\Phi_2} = X_p \quad (30)$$

where  $Z_p, X_p$  form the unitary operator basis for a *qudit* with  $p$  degenerate states  $\{|d\rangle\}$  ( $d = 1, 2, \dots, p$ ), such that  $Z_p|d\rangle = e^{i2\pi d/p}|d\rangle$  and  $X_p|d\rangle = |d-1 \bmod p\rangle$ . We now add a Josephson effect according to Eq. (29) to each of the two nodes (with Josephson energies  $\tilde{E}_{J1}$  and  $\tilde{E}_{J2}$ ). Note that this Josephson effect could have various origins: it could correspond to extra Josephson junction that is connected to a circuit containing an ideal gyrator (without intrinsic Josephson effect), or it could belong to the gyrating element, in case the latter is not ideal (and thus contains spurious Cooper-pair leakage). Using the representation in Eq. (30), we get the Hamiltonian

$$H = -\tilde{E}_{J1} \cos\left(\Phi_1 + \phi_1^{(\text{ext})} - \frac{2\pi}{p}n_2^{(\text{ext})}\right) - \tilde{E}_{J2} \cos\left(\Phi_2 + \phi_2^{(\text{ext})} + \frac{2\pi}{p}n_1^{(\text{ext})}\right), \quad (31)$$

which is easy to diagonalize. The resulting energy spectrum is shown in Fig. 3(b,c). It exhibits flux-fractionalization in the sense of a broken periodicity with respect to offset charge, depending on the value of  $p$ . The superposition of fractional flux and integer charge is further demonstrated by the fact that offset charges at node 1 and the offset fluxes at node 2 are linearly dependent. This superposition is insofar surprising as it seems (at least superficially) to go against usual gauge properties rooted in Maxwell's equations. Indeed, on a microscopic level, offset charges  $n_{\text{ext}}$  and fluxes  $\phi_{\text{ext}}$  correspond to applied voltages and magnetic fields, which are captured by the scalar and vector potentials  $\varphi$  and  $\mathbf{A}$ . Gauge transformations on those potentials are transformations  $\varphi, \mathbf{A} \rightarrow \varphi', \mathbf{A}'$ , which leave the resulting electric and magnetic fields invariant (i.e.,  $\mathbf{E} = -\nabla\varphi - \dot{\mathbf{A}} = -\nabla\varphi' - \dot{\mathbf{A}}'$  and  $\mathbf{B} = \nabla \times \mathbf{A} = \nabla \times \mathbf{A}'$ ). There are actually two separate seemingly paradoxical features, which can here be resolved thanks to the microscopic quantum geometric origin for the anyonic exchange mediated by a Chern number.

The first surprise concerns purely static fields. Namely, notice that in Fig. 3(a), we explicitly added two Josephson junctions in addition to the gyrator element. The two junctions form a loop, such that one may be tempted to argue that the resulting physics should not depend on  $\phi_1^{(\text{ext})}$  and  $\phi_2^{(\text{ext})}$  separately, but only on the loop phase  $\phi_1^{(\text{ext})} - \phi_2^{(\text{ext})}$ . This is not so for the Hamiltonian in Eq. (31), where both phases have their own distinct, measurable effect. Crucially, this feature does not break gauge invariance. If the gyrating element is a separate, additional device coupling to ground, see, e.g., Fig. 1(c), then the above physics is correct: the gyrator element and the two junctions do not form a single loop, but two distinct loops. Note however, that (as we already alluded to above) the gyrator element itself could also provide an *intrinsic* parasitic Josephson effect. In that case, there is no loop, and the phase dependence should vanish. Such a theory can also be constructed, this time by adding the phase shift  $\phi_z^{(\text{ext})}$  *globally* to all instances where the corresponding  $\phi_z$  appears in the Lagrangian (and not only to some parts, like  $\epsilon_0$ ). In other words, the above energy spectrum analysis in the presence of electromagnetic fields not only allows us to probe the exchange statistics, but also to distinguish different origins of the Josephson effect. The second surprise concerns the offset charges  $n_z^{(\text{ext})}$  due to applied gate voltages. Namely, with the identity  $\mathbf{E} = -\nabla\varphi - \dot{\mathbf{A}}$ , one would usually expect that offset charges can, via time-dependent unitary transformations, always be cast into time-dependent flux offsets (see also Refs. [74, 75] on that subject). This is (yet again) manifestly not so for the Hamiltonian given in Eq. (31). Overall, our approach reveals that various couplings to electromagnetic fields can be correct, and gauge invariance is not a property that can be imposed by simple a posteriori constraints on the effective low-energy theory. Instead, a correct description of the interaction with electric and magnetic

fields requires careful consideration of the details of the circuit. This microscopic approach is thus in contrast to common field theoretic descriptions of non-reciprocal interactions, such as for chiral edge states in the fractional quantum Hall effect [see also Eq. (5) and subsequent discussion], where gauge properties are commonly imposed heuristically.

A final comment regarding our use of the term flux fractionalization. This term has surfaced in other recent works dealing with superconducting rings and p-wave vortices [76–79] or in Kagome structures [80]. But this usage of the term refers generically to flux quantization in superconducting rings or vortices, which follows from the usual considerations of the superconducting condensate as a macroscopic coherent wave function, where the flux quantum depends on the effective charge of the condensate. Thus, in our language, this notion of fractional flux quantum would involve a change of the fundamental unit of *charge* carried by the condensate. We on the other hand observe the converse: fractionalization of the flux of a given excitation, which is visible when applying an electric (instead of magnetic) field.

## 7 Mapping to fermions

One particularly promising application for quantum hardware is the simulation of fermionic quantum many-body systems, typically described as

$$H = \sum_{z_1 z_2} h_{z_1 z_2}^{(2)} c_{z_1}^\dagger c_{z_2} + \sum_{z_1 z_2 z_3 z_4} h_{z_1 z_2 z_3 z_4}^{(4)} c_{z_1}^\dagger c_{z_2} c_{z_3}^\dagger c_{z_4}, \quad (32)$$

where the fermion operators  $\{c_z, c_{z'}^\dagger\} = \delta_{zz'}$  are cast into an appropriate basis. Such Hamiltonians are of great interest for quantum chemistry computations [38, 81], but also various solid state problems [39, 40, 82]. Generalizations from regular fermions to Majoranas further provide interesting connections to the SYK model [42, 83] and host so-called fracton excitations [84, 85].

Qubit-based quantum computational chemistry has been widely studied, and is considered one of the prime applications of near-term quantum hardware [38, 81]. While a Fock space representation allows for a straightforward state initialization [86], there usually remains the well-known problem of fermions statistics. The anticommutation already causes problems for classical computation methods such as the famous sign problem in quantum Monte Carlo methods [87]. Specifically for digital quantum hardware simulations [43], anticommutation properties require strongly non-local quantum gates, due to the Jordan-Wigner mapping from fermion operators to the qubit (Pauli) operators [88], which in turn necessitates quantum algorithms of prohibitively large depth (upon sequential application of universal gates) for currently (or near future) available NISQ devices [89]. As a consequence, the nonlocality of Jordan-Wigner chains has led to the development of more efficient (but still nonlocal) encodings of anticommutation properties [90, 91] or to sophisticated techniques for increasing the simultaneity of qubit gates [92–96].

In contrast, the here presented many-body quantum geometric mechanism provides a direct mapping from scalar fields to fermionic Hamiltonians [Eq. (32)], which permits the use of *local* interactions and control.

To start, take a generic circuit with  $Z$  nodes (recall that  $Z$  is even), and set each first Chern number equally to the value 2, i.e.,  $C_{zz'}^{(1)} = 2$  (for  $z' > z$ ). In accordance with Eq. (18) and the subsequent discussion, we here find an exchange statistics of  $p = 2^{Z/2}$  and (again with  $z' > z$ )  $q_{zz'} = (-1)^{z+z'} 2^{Z/2-1}$  [where  $(-1)^{z+z'}$  simply provides an alternating sign depending on the  $z$  and  $z'$  indices, due to the Levi-Civita tensor in Eq. (20)]. Ultimately, all pairs of nodes need to be connected to form a complete graph, see, e.g., Fig. 1. We thus observe the following. The lowest Landau level has  $p = 2^{Z/2}$ -fold degeneracy. Moreover, all exchange ratios simplify to

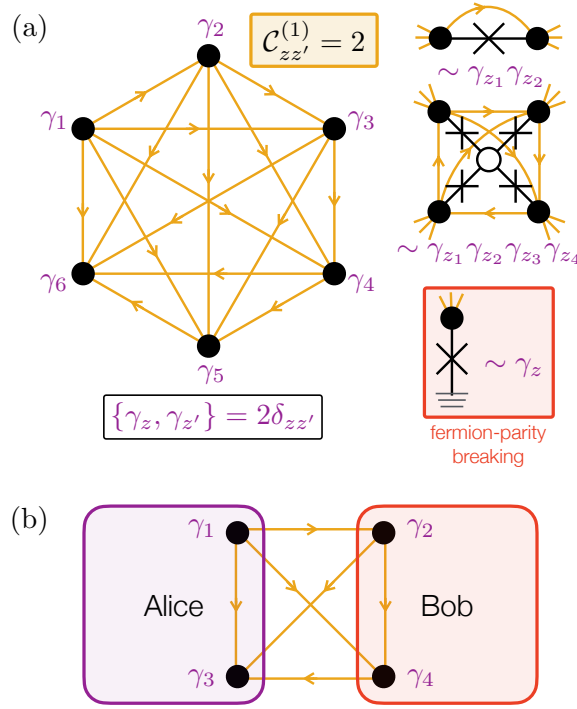


Figure 4: Mapping from Chern networks to fermionic systems. (a) Choosing all Chern numbers identically equal 2 (in a complete graph) reduces the anyons to regular (Majorana) fermions. Quadratic and quartic interaction terms are equivalent to two-terminal, respectively 4-terminal Josephson couplings. Note that with Josephson couplings to ground (which do not conserve the total Cooper pair charge on the nodes) the circuit architecture allows for the generation of terms in the Hamiltonian which break the fermion-parity superselection rule. (b) Fermion-parity breaking implies a breaking of the no-signalling theorem, which can be probed by two participants (Alice and Bob) having access to the fermionic nodes.

$q_{zz'}/p = \pm 1/2$ , such that the anyons  $e^{i\Phi_z}$  anticommute, and for the same reason  $(e^{i\Phi_z})^2 = e^{i2\Phi_z}$  must be a c-number (which, upon appropriate choice of the offset phase contributions, can be set to 1). The system thus generates a set of  $Z$  real Majorana fermions,

$$e^{i\Phi_z} \equiv \gamma_z \quad (33)$$

with  $\{\gamma_z, \gamma_{z'}\} = 2\delta_{zz'}$ . Since  $Z$  is even, we can always represent these  $Z$  Majoranas in terms of  $Z/2$  ordinary complex fermions, and thus open the road towards implementations of the Hamiltonian in Eq. (32). To this end, we introduce the well-known mapping between the Majorana basis and the actual fermion basis, by choosing the representation

$$\begin{aligned} \gamma_z &= c_z + c_z^\dagger, \\ \gamma_{z+Z/2} &= i(c_z - c_z^\dagger), \end{aligned} \quad (34)$$

where the  $z$  index range is cut in half,  $z = 1, \dots, Z/2$ , when referring to fermions instead of Majoranas. This mapping is not unique. Any  $SO(Z)$  transformation applied to  $\gamma_z$  still results in the same the fermionic algebra.

In order to get a nonzero coupling between the fermions, i.e., to get to the actual form of Eq. (32), we again need a nonzero  $H_J$ . Importantly, in order to get to a regular fermionic field, we need to *restrict*  $H_J$ . Namely, we can only allow  $H_J$  which conserves the total kinetic charge  $N_{\text{tot}} = \sum_z N_z$ , i.e.,  $[H, N_{\text{tot}}] = [H_J, N_{\text{tot}}] = 0$ . This is the case when  $\delta A_z$  and  $\epsilon_0$  (which, as a

remainder, are both periodic in  $\phi_z$ ) depend only on phase differences,  $\phi_z - \phi_{z'}$ . In that case, the only Fourier components in  $\epsilon_0$  and  $\delta A_z$ , see also Eq. (26), are the ones where  $\sum_z m_z = 0$ . If we now project  $H_J$  onto the lowest Landau level  $e^{i\phi_z} \rightarrow e^{i\Phi_z}$  (as developed in the previous section), and use above mapping to Majoranas, we arrive at a Hamiltonian of the form

$$H = \sum_{z_1 z_2} \tilde{h}_{z_1 z_2}^{(2)} \gamma_{z_1} \gamma_{z_2} + \sum_{z_1 z_2 z_3 z_4} \tilde{h}_{z_1 z_2 z_3 z_4}^{(4)} \gamma_{z_1} \gamma_{z_2} \gamma_{z_3} \gamma_{z_4} + \dots \quad (35)$$

The reason that we only get even terms is due to  $N_{\text{tot}}$  being conserved. In the superconducting circuit language, the term  $\sim \tilde{h}^{(2)}$  (regular, bilinear fermion tunneling) corresponds to transporting single Cooper pairs, whereas two-body interactions  $\sim \tilde{h}^{(4)}$  correspond higher order tunneling processes (e.g., Cooper pair co-tunneling, or quartet physics). Note further that Eq. (35) is more general than Eq. (32), as it also allows the inclusion of pairing,  $\sim c_z^\dagger c_{z'}^\dagger$ . As already foreshadowed, the Majorana Hamiltonian with quartic interactions ( $\sim \tilde{h}^{(4)}$ ) was recently studied in connection with so-called fracton excitations [84, 85]. If the quartic term dominates and its elements take random values, it falls into the area of the applicability of the SYK model [42, 83]. This demonstrates the mapping from a generic compact scalar field to a wide variety of important known problems.

## 8 Breaking Wigner superselection rule

Crucially, we can also map to yet unexplored field theories with unsettling properties. As a first example, we keep the above Chern number matrix, with  $C_{zz'} = 2$  (for  $z > z'$ ), such that the anyons reduce to Majorana fermions as demonstrated above. But now, we no longer restrict  $H_J$  to conserve  $N_{\text{tot}}$ , i.e., the energy  $\epsilon_0$  and vector potentials  $\delta A_z$  are now allowed to have an arbitrary (yet still periodic) dependence on all phases  $\phi_z$ , thus now allowing  $\sum_z m_z \neq 0$  for the Fourier components. Crucially, at the very least for physical implementations via superconducting circuits, this case is the *default scenario*, since coupling to ground is a physical possibility, and in many cases unavoidable. Consequently, circuits without targeted suppression of Josephson leakage to ground generically map onto Hamiltonians of the form

$$H = \sum_{z_1} \tilde{h}_{z_1}^{(1)} \gamma_{z_1} + \sum_{z_1 z_2} \tilde{h}_{z_1 z_2}^{(2)} \gamma_{z_1} \gamma_{z_2} + \sum_{z_1 z_2 z_3} \tilde{h}_{z_1 z_2 z_3}^{(3)} \gamma_{z_1} \gamma_{z_2} \gamma_{z_3} + \dots \quad (36)$$

A contact to ground thus provides *linear* terms in the Hamiltonian,  $\sim \sum_z h_z^{(1)} \gamma_z$  (with  $h_z^{(1)}$  real), or even cubic terms ( $\sim h^{(3)}$ ). While such terms are perfectly Hermitian, they clearly break the fermion parity superselection rule [47], also referred to as Wigner superselection. As just indicated, on a physical level, we can connect the breaking of the Wigner superselection rule to charge conservation on the circuit. To the best of our knowledge, there exists no literature attempting to analyze even the basic properties of Hamiltonians of the above type, let alone investigate possible quantum phase transitions or other collective phenomena, since parity-breaking terms  $\sim h^{(1,3)}$  were not expected to exist in nature. Our work thus very organically unravels the existence of an entirely unexplored class of quantum field theories—calling for a dedicated future research effort to explore or extend quantum field theoretic methods to tackle parity-breaking fermionic systems (and anyonic generalizations thereof).

Let us defuse right away any concerns that our theory might violate fundamental laws of nature. The backbone of the Hamiltonian in Eq. (7) are the set of ground states of  $H_0$  for all  $\phi_z$ ,  $|0(\{\phi_z\})\rangle$ . If we assume a superconducting circuit realization of the system,  $H_0$  is formulated as a regular, fermion-parity-conserving theory (which must be true on some level for any field theory based on electronic degrees of freedom). Then  $|0(\{\phi_z\})\rangle$  preserves fermion-parity superselection for the underlying electrons, independent of the values of the set

$\{\phi_z\}$ . The low-energy theory in Eq. (7) merely provides many-body wave-function solutions that are coherent superpositions of the states  $|0(\{\phi_z\})\rangle$  with  $\phi_z$ -dependent amplitudes. Hence any low-energy pair of states  $|\psi\rangle$  and, e.g.,  $c_z^\dagger|\psi\rangle$  [see Eq. (34)] both have the same fermion-parity in terms of the original (microscopic) electronic degrees of freedom. The fermion-parity breaking property only appears in the new set of *emergent* anyonic excitations satisfying Eq. (17), due to the Landau level physics on the closed torus manifold.

The here observed fermion-parity breaking is therefore conceptually very similar to implementations of fermionic operators in terms of universal qubit hardware. However, we again have to insist that the latter requires highly non-local gates (such as Jordan-Wigner chains [43, 88]) in order to recreate the anticommuting property. Our theory on the other hand is (to the best of our knowledge) the first to implement a fermion-parity breaking theory with local gates. And it is exactly this difference between local and nonlocal fermionic gates, which is of quite some conceptual interest.

To appreciate this point, we refer to a prominent emerging fundamental research area, which strives to derive the axioms of quantum mechanics not from physical principles, but from a quantum information point of view [8–10, 97–99]. Within this research thrust, there has been quite some debate as to whether Wigner superselection in fermionic systems requires physical, relativistic arguments, or whether it can be justified in a non-relativistic setting, by fundamental quantum-information theoretic axioms, such as local realism (in the quantum mechanical sense) [11, 12, 100, 101].

Importantly, our theory provides a counter-example of a theory that breaks Wigner superselection, and thus allows for the formulation of protocols which demonstrably break the no-communication theorem. This breaking of local realism does not break relativistic principles, since our theory relies on integrating out the photon degrees of freedom (which propagate at the speed of light). Nonetheless, if one were to impose no-signalling without explicitly invoking relativistic arguments [101], one would have erroneously excluded the possibility that a theory like the one presented here exists in the first place.

In the Appendix C, we present a circuit realization of a simple but elegant protocol presented in Ref. [101], which demonstrates how breaking Wigner superselection allows for changing the outcome of a measurement in one subsystem (Alice), by only performing local gates in another, spatially separated subsystem (Bob). This protocol requires only two actual fermionic modes (one for Alice, one for Bob), such that it can be run on a circuit with 4 Majorana nodes.

Overall, this protocol kills two birds with one stone: it provides a smoking gun experimental signature for the presence of anticommuting (fermionic) excitations, as well as a breaking of the no-communication theorem, opening the door towards all-to-all quantum gates. Moreover, we note that precision in the gate operations is not required, and similarly, the suppression of errors is not critical for a successful probing of the sought-after effect. To the contrary, this experiment is highly sensitive to any ever so slight breaking of fermion parity.

## 9 Non-identical anyons

We again stress that the above connection between locality and charge conservation holds if all Chern numbers in the complete graph are the same,  $C_{zz'} = C$  (for  $z > z'$ ). For the above discussed case of  $C = 2$ , we get emergent Majorana fermions, and thus recover the original, fermionic Wigner superselection if  $\sum_z N_z$  is conserved. This superselection principle generalizes to parafermions for  $C > 2$  (where, as already stated, we get parafermion operators  $\eta_z \equiv e^{i\Phi_z}$  with  $\eta_z^C = 1$ , and  $\eta_z\eta_{z'} = e^{i2\pi/C}\eta_{z'}\eta_z$ ). Independent of the value of  $C$ , the exchange statistics do not depend on  $z, z'$  – a property we refer to as the anyons being identical. If we

still impose the same charge conservation constraint on the full  $H$  (for  $C > 2$ , that is), we get after projection onto the lowest Landau level a Hamiltonian of the form,

$$H = \sum_{z_1 z_2} h_{z_1, z_2} \eta_{z_1}^\dagger \eta_{z_2} + \sum_{z_1 z_2 z_3 z_4} h_{z_1 z_2 z_3 z_4}^{(4)} \eta_{z_1}^\dagger \eta_{z_2}^\dagger \eta_{z_3} \eta_{z_4} + \dots \quad (37)$$

The generalized parity operator [102] (also called symmetry generator) can be defined as

$$Q = \prod_{z=1}^{Z/2} \eta_{2z-1}^\dagger \eta_{2z} \quad (38)$$

guaranteeing  $Q^\dagger \eta_z Q = e^{i2\pi/C} \eta_z$  for all  $z$  ( $Q$  is unitary). Consequently, for above charge conserving Hamiltonian,  $Q^\dagger H Q = H$ , establishing  $Q$  as a generalized conserved parity operator. This again leads to a no-signalling theorem, if we demand that no unitary operation nor measurement between any two spatially separate participants (commonly called Alice and Bob) can generate superpositions of states with different eigenvalues of  $Q$ . Indeed, with above concrete physical platform, limiting operations and measurements to charge conserving processes, and (optionally) gate operations involving charge and flux shifts, the generalized Wigner superselection (anchored to  $Q$ ) remains conserved for all possible communication experiments that can be run on that hardware. Of course, if we once again relax the charge conservation constraint (leading to non-bilinear terms in  $H$ , see also previous section), the no-signalling theorem can be broken again.

Crucially, no-signalling breaks down even in the presence of charge conservation – if we make the Chern numbers unequal. Here, defining the generic anyon  $\eta_z = e^{i\Phi_z}$ , we simply recover the exchange statistics given by Eq. (17), with an exchange phase that now depends on  $z$  and  $z'$ , via  $q_{zz'}$ . We refer to particles satisfying such statistics as *non-identical* anyons. While a charge conserving theory still maps onto a Hamiltonian of the form of Eq. (37), this theory is no longer local. This fact can be shown in a quantum communication language (not necessarily referring to a specific Hamiltonian). Let us partition the  $Z$  nodes into two spatially separated regions,  $Z_A$  and  $Z_B$  (in reference to Alice and Bob), that is, a region with  $z = \{1, \dots, Z_A\}$  and another region  $z = \{Z - Z_B + 1, \dots, Z\}$  ( $Z = Z_A + Z_B$ ). Let Alice and Bob perform either unitary operations  $U_A = U_0 e^{iA}$  and  $U_B = V_0 e^{iB}$  ( $A$  and  $B$  are Hermitian operators, whereas  $U_0$  and  $V_0$  are unitary) or measurements on Hermitian operators  $M_A$  and  $M_B$ . Assuming yet again that we have only charge conserving operations and charge/flux shifts at our disposal, we can restrict unitaries and measurements as follows: we impose that neither unitary operations nor projective measurements can create states that give rise to superpositions of states with different charge  $N_{\text{tot}}$ . We can simply call this a charge superselection rule (which reduces to the Wigner superselection rule for the initially discussed fermionic case). Projecting this constraint onto the lowest Landau level, this restricts all Hermitian operators ( $A$  and  $B$  as well as  $M_A$  and  $M_B$ ) to have the same expansion as the Hamiltonian in Eq. (37). The unitaries  $e^{iA}$  and  $e^{iB}$  can thus not change the total charge of the system. This is too restrictive for unitary operations, since, as just explained, charge superselection only requires there to be no *superpositions* of different charge states after the operation, but charge does not need to be conserved as such. We therefore include in our definition of  $U_A$  and  $U_B$  the “prefactor” unitaries  $U_0$  and  $V_0$ , respectively. Those can be of the form of products  $U_0 = \prod_z e^{i\alpha_z \Phi_z}$  and  $V_0 = \prod_z e^{i\beta_z \Phi_z}$ , respectively, with integer  $\alpha_z$  and  $\beta_z$ . If we had *identical* anyons,  $q_{zz'} = q$  for all  $z > z'$ , locality ( $U_A$  and  $M_A$  only contains  $\eta_z$  with  $z = 1, \dots, Z_A$ , whereas  $U_B$  and  $M_B$  only contains  $\eta_z$  with  $z = Z - Z_B + 1, \dots, Z$ ) would guarantee that unitaries and measurements on Alice’s side commute with the ones on Bob’s side. As soon as we allow for *non-identical* anyons,  $q_{zz'}$  dependent on  $z, z'$ , they no longer commute, allowing for signalling at a distance, breaking common notions of locality.

Overall, we have two versions of locality breaking. Either we have identical anyons, and allow the breaking of charge superselection (defined on the original boson field), or we consider non-identical anyons, where locality breaks irrespective of whether or not charge superselection is present. Let us as a final remark point out that the former of the two situations can actually be treated on the same footing as the latter. Namely, as explained in detail above, charge conservation can be broken by couplings to ground. In the original language of the scalar field, those terms emerge due to Fourier components in  $\epsilon_0$  and  $\delta A_z$ , see Eq. 26, where  $\sum_z m_z \neq 0$ . We can nominally include ground by performing a global shift of all  $\phi_z$  with a global scalar  $\phi_z \rightarrow \phi_z - \phi_0$  – the usual  $U(1)$  gauge related to charge conservation. We can now even endow ground with a finite (though very large) capacitance on the level of Eq. (6), which allows us to keep track of the number of charges that are exchanged with ground, by elevating the ground phase  $e^{i\phi_0}$  from a scalar to an operator. Thus, for identical anyons ( $C_{zz'} = C$ ), any unpaired Majorana- or parafermion operator [for Majoranas, see odd terms in Eq. (36)] receives an additional “counting field” operator,  $\eta_z \rightarrow \eta_z e^{-i\phi_0}$ , keeping track of the overall charge on the system including ground. However, since there are no Chern connections (gyrators) between the nodes and ground,  $e^{i\phi_0}$  commutes with all  $\eta_z$ , and thus cannot salvage locality. We can think of the ground phase operator  $e^{i\phi_0}$  as yet another particle (located on ground as an additional node), which corresponds to a special case of a *non-identical* particle, as it does not have the same (fermionic or parafermionic) exchange statistics.

## 10 Conclusions and outlook

### 10.1 Conclusions

In this work, we demonstrated that geometric (Berry curvature) terms in generic conventional superconducting multiterminal junctions give rise to excitations with anyonic exchange statistics. The fractional exchange phase  $\sim q/p$  is linked to the nonzero Chern numbers of the system, and can take in principle any rational value, such that there emerge Majoranas or even more general types of parafermions. The fractional exchange statistics can be measured by a periodicity breaking of the Aharonov-Casher phase, which is associated to a fractional flux carried by the excitations. Due to the emergent anyonic exchange statistics, the here considered system allows direct implementation of a simulation of fermionic systems with *local* gate operations, relevant for a number of important problems, such as quantum computational chemistry.

Our work also provides a number of insights of fundamental nature. In addition to the obvious analogy with the fractional quantum Hall effect, we particularly highlighted the fact that there naturally occur interactions with *non-identical* anyons, ultimately yielding a lattice quantum theory that breaks fermion-parity superselection rule, and generalizations thereof for anyons. This effect can be related on a circuit level to the breaking of charge conservation with respect to ground. In contrast to other known parity breaking effects (as in implementations of fermionic gates in qubit hardware via non-local Jordan-Wigner chains), the local nature of the fermionic gates allowed us to connect our work to the ongoing endeavour to derive quantum mechanics from an information-theoretic point of view, indicating the importance of relativistic arguments in order to satisfy the no-communication constraint.

### 10.2 Outlook

By including geometric interactions in generic many-body lattice systems, we lay the groundwork towards a different flavour of quantum information hardware, where the fundamental information unit is an anyonic qudit. Beyond applications, the here developed theory presents

a whole host of important open questions of fundamental nature. For instance, the aforementioned breaking of fermion-parity superselection rules (and anyonic generalizations thereof) stipulates that the understanding of networks with quantum geometric interactions involves solving a class of quantum field theories which have so far hardly been examined, as they were not expected to be realized in nature. Take for concreteness the ordinary Hubbard model, which can be realized in circuits with charge-conserving Josephson effects, see Eq. (32). We would for instance deem it highly interesting to investigate if the known phenomenology, such as the phase diagram (for which, incidentally, there still does not exist full consensus [103]), survives the addition of (even weak) fermion-parity breaking processes. Note that this is as much a physical question as it is a computational one: the success of many numerical techniques for solving strongly correlated model systems, such as DMRG [104], is connected to entanglement entropy area laws [105], and is known to work best when the ground state is sufficiently close to being a product state [106], which we expect not to be the case for superpositions of states with different fermion parity.

There furthermore exist quite a number of open research directions in relationship to the fractional quantum Hall effect. In this context, we reemphasize that our setup can realize a reduced (i.e., scalar) version of Chern-Simons theory, with a number of special properties, most notably the absence of a bulk in the proper sense (the Chern number is defined within the node degrees of freedom itself), and the possibility of a spatially varying Chern level, which is at the origin of the Wigner superselection breaking. In an upcoming work, we study deepen the understanding of the here present radical change of the usual bulk-boundary correspondence, yielding an access point to a so far unexplored notion of *hollow* topological matter.

## Acknowledgements

We warmly thank Fabian Hassler, David DiVincenzo, Markus Müller, Maarten R. Wegewijs, Frank Wilhelm-Mauch, Z. Leghtas, P. Campagne-Ibarcq, J.-D. Pillet, L. Bretheau, and Janine Splettstoesser for fruitful discussions. R.M. would like to thank Julia Meyer for her insights and for directing us to relevant literature.

**Funding information** This work has been funded by the German Federal Ministry of Education and Research within the funding program Photonic Research Germany under the contract number 13N14891.

## A Cavity Chern insulator with charge qubit coupler

The standard Chern insulator Hamiltonian in a 2D lattice is given as

$$H_{\text{CI}} = [\delta + \cos(\phi_1) + \cos(\phi_2)]\sigma_z + \sin(\phi_1)\sigma_x + \sin(\phi_2)\sigma_y. \quad (39)$$

For simplicity, above Hamiltonian is unitless. We are free to multiply the entirety of  $H_{\text{CI}}$  with a total energy scale  $h$ , i.e.,  $H_{\text{CI}} \rightarrow hH_{\text{CI}}$ . This Hamiltonian is well-known to exhibit topological gapped phases for  $|\delta| < 2$ , with Chern number  $\pm 1$  (defined in  $\phi_1$  and  $\phi_2$ ).

Let the above be our target Hamiltonian that we seek to implement with the photonic degrees of freedom of a quantum optical cavity. Specifically, if we use two cavity modes  $b_1^{(\dagger)}$  and  $b_2^{(\dagger)}$ , see also right panel in Fig. 1c, we can reverse engineer above Chern insulator Hamiltonian

via the bosonic cavity Hamiltonian

$$H_{\text{cavity}} = \tilde{\delta}\sigma_z + \frac{b_1 + b_1^\dagger}{2}\sigma_z + \frac{b_2 + b_2^\dagger}{2}\sigma_z + i\frac{b_1 - b_1^\dagger}{2}\sigma_x + i\frac{b_2 - b_2^\dagger}{2}\sigma_y \quad (40)$$

$$+ u_{K1}(b_1^\dagger b_1 - \mu_1)^2 + u_{K2}(b_2^\dagger b_2 - \mu_2)^2 + u_{cK} b_1^\dagger b_1 b_2^\dagger b_2.$$

The second line contains the free boson Hamiltonian with auto- and cross-Kerr terms ( $u_{K1}$  and  $u_{K2}$ , respectively,  $u_{cK}$ ) representing the boson many-body interactions within the cavities (auto-Kerr) and between the two cavities (cross-Kerr). The offsets (chemical potentials)  $\mu_{1,2}$  can be suitably tuned by an ac drive to the individual cavities. The logic is now as follows. By tuning  $\mu_{1,2}$  to large values, we can drive the cavities to a high-photon population state,  $n_{1,2} = b_{1,2}^\dagger b_{1,2} \gg 1$ . In that regime, the boson operators can be approximated as  $b_{1,2} \approx \sqrt{n_{1,2}} e^{-i\phi_{1,2}}$ , thus mapping from Eq. (40) to Eq. (39). Note that in these two Hamiltonians, the amplitude of the  $\sigma_z$  term is rescaled ( $\delta$  versus  $\tilde{\delta}$ ). This rescaling is necessary to account for the population prefactor  $\sim \sqrt{n_{1,2}}$  when replacing the boson ladder operators with the phase operators.

The remaining challenge now is to show that a suitably designed capacitive and inductive coupling between a given cavity mode and, e.g., a charge qubit can implement all necessary interaction terms, given in the first line of Eq. (40). We consider an ordinary flux-tunable charge qubit, with a dc-SQUID composed of two Josephson junctions, shunted by a capacitance, as shown in Fig. 1c. Let us for simplicity start by considering a single cavity with modes  $X = (b + b^\dagger)/\sqrt{2}$  and  $P = i(b - b^\dagger)/\sqrt{2}$ , representing the electro-magnetic charge and flux of the cavity, respectively. A generic capacitive and inductive coupling between cavity and charge qubit yields the Hamiltonian

$$H_{cc} = E_C \left( n + n_{\text{ext}} + \frac{\mu}{E_C} \hat{X} \right)^2 - (E_J + 2\nu\hat{P}) \cos \left( \varphi + 2\frac{\lambda}{E_J} \hat{P} \right). \quad (41)$$

The charge qubit (with charge and phase  $[\varphi, n] = i$ ) is modelled with the following parameters: the capacitive energy  $E_C$  and the total Josephson energy  $E_J$  of the SQUID (which is tunable by an externally applied flux). The capacitive (charge-charge) coupling is parametrized by the energy scale  $\mu$ . The inductive (current-current) coupling enters twice: once in an offset of the Josephson cosine energy (with the energy scale  $\lambda$ ), and a second time as a dynamical rescaling the Josephson energy itself (proportional to  $\nu$ ). We tune the offset charge  $n_{\text{ext}}$  close to the charge degeneracy point, and operate the charge qubit close to the Cooper pair box regime ( $E_C > E_J$ ). For instance, for  $n_{\text{ext}} = -1/2 + \delta n_{\text{ext}}$  ( $\delta n_{\text{ext}} \ll 1$ ), the two (nearly) degenerate charge states are  $n = 0, 1$ , forming the charge qubit basis with the Pauli operators  $n - 1/2 \rightarrow \sigma_z/2$ ,  $\cos(\phi) \rightarrow \sigma_x/2$ , and  $\sin(\phi) \rightarrow \sigma_y/2$ . Projected onto that qubit basis (and up to linear order in all couplings  $\mu, \nu, \lambda$ ), we get

$$H_{cc} \approx \tilde{\delta}\sigma_z - \tilde{\gamma}\sigma_x + \mu\sigma_z X - \nu\sigma_x P + \lambda\sigma_y P, \quad (42)$$

where  $\tilde{\delta} = E_C \delta n_{\text{ext}}$  and  $\tilde{\gamma} = E_J/2$ . Tuning sufficiently far off resonance, such that  $\tilde{\delta}$  is larger than  $\tilde{\gamma}$ , we are almost at the desired shape. Now, we include two cavities instead of one,  $X, P \rightarrow X_{1,2}, P_{1,2}$ . In lowest order in the coupling, the interactions between charge qubit and the two cavities is simply additive, yielding

$$H_{cc} \approx \tilde{\delta}\sigma_z + \sum_{j=1,2} [\mu_j \sigma_z X_j - \nu_j \sigma_x P_j + \lambda_j \sigma_y P_j]. \quad (43)$$

All that remains is to tune the couplings to values  $\mu_1 \approx \nu_1 \approx \mu_2 \approx \lambda_2 \approx 1$  and  $\lambda_1 \approx \nu_2 \approx 0$  to arrive at the target Hamiltonian given in Eq. (40). This concludes the engineering of a Chern insulator in the 2D lattice space defined by the photon numbers of two cavities.

## B Gauges for Uniform Magnetic Field on Torus

As noted in the main text, usual gauge choices for vector potentials in the extended 2D plane are at risk of yielding inconsistent results when embedded on a compact manifold, such as the torus. We here clarify certain gauge aspects for said torus, by means of a numerical investigation. We discretize the torus with a mesh of  $N \times N$  points, as shown in Fig. 5. The Hamiltonian resulting from Eq. (3) (under appropriate inclusion of capacitive coupling) can be numerically implemented as the single-particle Hamiltonian hopping between the points on the mesh, and the effective magnetic field can be implemented as the phase acquired along the movement between the neighbour points.

Thus, the Berry connection in this discretized model is described by the values  $A_{n,m}^x = \int_{x_n}^{x_{n+1}} A_x(x, y_m) dx$  and same formula for  $A_{n,m}^y$  with  $x \leftrightarrow y$ , and fluxes through the unit cell  $\tilde{\mathcal{B}}_{nm} = \int_{x_n}^{x_{n+1}} \int_{y_m}^{y_{m+1}} \tilde{\mathcal{B}}(x, y) dx dy$ . Here, to simplify the notation, we denote  $x = \phi_1$ ,  $y = \phi_2$ . Periodic boundary conditions are implemented by using cyclic indices  $n, m$ , that is, they are set to 0 when they assume the value  $N$ . The constant magnetic field  $\mathcal{B}$  is implemented through the condition

$$\tilde{\mathcal{B}}_{nm} = A_{n,m}^x + A_{n+1,m}^y - A_{n,m+1}^x - A_{n,m}^y, \quad (44)$$

$$\exp\{i\tilde{\mathcal{B}}_{nm}\} = \exp\{i(2\pi/N)^2\mathcal{B}\}, \quad (45)$$

where  $\tilde{\mathcal{B}}_{nm}$  is basically the flux through the elementary cell. The exponentiation of the phases relates the values up to the  $2\pi$ , giving us the relation

$$\tilde{\mathcal{B}}_{nm} = (2\pi/N)^2\mathcal{B} - 2\pi\mathcal{K}_{nm}, \quad \mathcal{K}_{nm} \in \mathbb{Z}. \quad (46)$$

On the other side, using the definition of  $\tilde{\mathcal{B}}_{nm}$  and cyclic indices, we get  $\sum_{\forall n,m} \tilde{\mathcal{B}}_{nm} = 0$ , which naturally follows from Stokes theorem on the torus. This condition results in the quantization of the magnetic field

$$2\pi\mathcal{B} = \sum_{\forall n,m} \mathcal{K}_{nm} = \mathcal{C} \in \mathbb{Z}, \quad (47)$$

where  $\mathcal{C}$  is the Chern number. Here, the most trivial example is when all ‘‘horns’’  $\mathcal{K}$  (see also main text) are gathered into a single one at  $(n_0, m_0)$ , i.e.  $\mathcal{K}_{nm} = 0$  everywhere except for  $\mathcal{K}_{n_0 m_0} = \mathcal{C}$ . Then, for example a linear gauge can be constructed in the following way:

$$\begin{aligned} A_{n_0, m \leq m_0}^x &= -\frac{2\pi\mathcal{C}}{N}m, & A_{n_0, m > m_0}^x &= -\frac{2\pi\mathcal{C}}{N}m + 2\pi\mathcal{C}, \\ A_{n \leq n_0, m}^y &= \frac{2\pi\mathcal{C}}{N^2}n, & A_{n > n_0, m}^y &= \frac{2\pi\mathcal{C}}{N^2}n - \frac{2\pi\mathcal{C}}{N} \end{aligned} \quad (48)$$

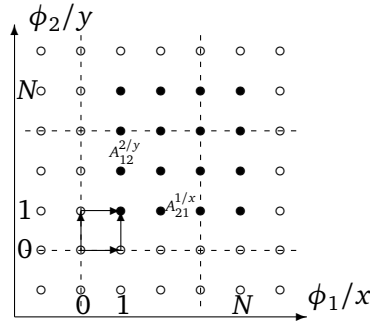
which is also illustrated in Fig. 6.

This discrete gauge in the continuous limit takes the following form

$$\begin{aligned} A^x(x, y) &= -\mathcal{C}\delta(x - x_0)(y - 2\pi\theta(y - y_0)), \\ A^y(x, y) &= \frac{\mathcal{C}}{2\pi}(x - 2\pi\theta(x - x_0)), \\ \tilde{\mathcal{B}}(x, y) &= \frac{\mathcal{C}}{2\pi} - 2\pi\mathcal{C}\delta(x - x_0)\delta(y - y_0), \end{aligned} \quad (49)$$

where  $\delta(x) = \theta'(x)$  denotes a  $2\pi$  periodic Dirac delta function, and the  $\theta(x)$  is an extended step function, i.e., not a single step, but a ladder, with steps at  $-2\pi, -\pi, 0, 2\pi, 4\pi$ , and so on.

Numerical diagonalization of the Hamiltonian given in Fig. 5 for the case  $\mathcal{C} = 2$  illustrates the predicted  $\mathcal{C}$ -fold degeneracy of the lowest Landau level on the torus in the main text, see



$$H = e^{iA_{nm}^x} |n+1, m\rangle \langle n, m| + e^{iA_{nm}^y} |n, m+1\rangle \langle n, m| + h.c.$$

Figure 5: Discretization of the Fock space of two superconducting islands. The mesh is defined on a torus, i.e. index  $N \equiv 0$ .

Fig. 6(b), left. On the right-hand side of Fig. 6(b), the probability distribution of the wave function is shown. Here one may notice an important feature. Despite the problem being translational invariant, the physical part of the solution, which is the probability, is not. The wave function has a maximum, and its position is not related to the “horn”, which proves that the “horn” does not affect the measurable part of the solution. But the phase of the wave function is, of course, affected by the gauge. This issue arises from the fact that the gauge invariance means that all fluxes remain the same. In the case of the torus it adds two different types of closed trajectories, for example the loops  $\mathcal{W}_z$  and  $\mathcal{W}_{z'}$  shown in Fig. 2(b) [in our case  $z = 1$  and  $z' = 2$ ]. Thus, we need to fix the values for the fluxes through these loops too. Modifying the gauge, we found the correlation between these fluxes and the solution: the maximum of the wave function coincides with the crossing of the straight trajectories  $\mathcal{W}_1$  and  $\mathcal{W}_2$ , position of which chosen such that the fluxes through these both trajectories are equal to zero (up to  $2\pi$  addition, of course), see the grey lines in Fig. 6(b), right.

## C Protocol to probe violation of no-communication theorem

As pointed out in the main text, Ref. [101] introduces a simple protocol which demonstrates how breaking Wigner superselection allows for changing the outcome of a measurement in one subsystem (Alice), by only performing local gates in another, spatially separated subsystem (Bob). We first reiterate the protocol as given in Ref. [101], and then we show how it is implemented within the circuit hardware.

The protocol only requires two fermionic modes,  $a, a^\dagger$  for Alice, and  $b, b^\dagger$  for Bob, such that  $\{a, a^\dagger\}_+ = \{b, b^\dagger\}_+ = 1$ , whereas  $\{a, b^\dagger\}_+ = 0$  (due to the two modes being spatially separated). Starting from the vacuum state  $|0\rangle$  ( $a|0\rangle = b|0\rangle = 0$ ), we first prepare the initial state with a unitary gate performed by Alice,  $U_A = (1 - a + a^\dagger)/\sqrt{2}$ . This gate is designed to explicitly break Wigner superselection, since the initial state after the gate reads,

$$|\psi_A\rangle = U_A|0\rangle = \frac{|0\rangle + a^\dagger|0\rangle}{\sqrt{2}}. \quad (50)$$

We now imagine that Alice performs a local measurement with the observable  $O_A = a + a^\dagger$ , which yields,

$$\langle \psi_A | O_A | \psi_A \rangle = 1. \quad (51)$$

If, before Alice’s measurement of  $O_A$ , we allow Bob to perform a gate of the form  $U_B = b + b^\dagger$ ,

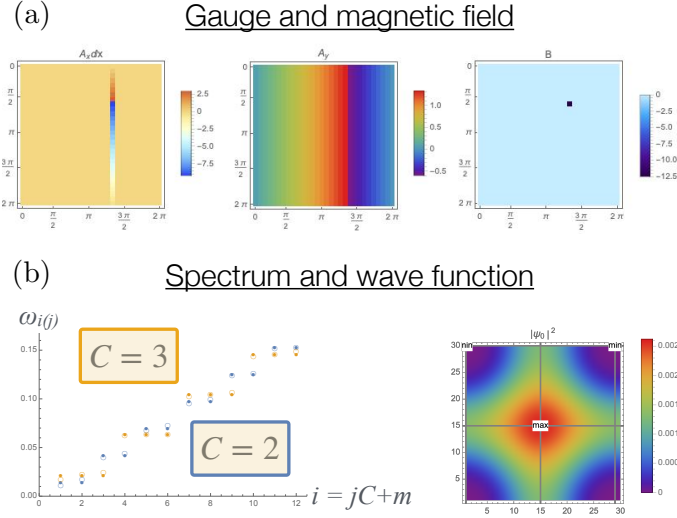


Figure 6: (a) An example of the linear gauge. In the left plot the phase is scaled by  $dx = 2\pi/N$ . In the right plot one can clearly see the “horn” in the magnetic field. (b) The numerical solution for the Hamiltonian given in the Fig. 5. On the left is the spectrum with a distinct degeneracy for each Landau level. The blue and yellow circles (solid) represent the cases of the degenerate Landau levels for  $C = 2$  and  $C = 3$ , respectively. When adding Josephson junctions, the degeneracy is lifted (empty circles). On the right is the wave function probability. Grey lines correspond to the topologically non-trivial straight loops with zero flux through them.

yielding the state  $|\psi_{AB}\rangle = U_B U_A |0\rangle$ , the subsequent measurement on Alice’s side would yield

$$\langle \psi_{AB} | O_A | \psi_{AB} \rangle = -\langle \psi_A | O_A | \psi_A \rangle = -1, \quad (52)$$

which is manifestly different from the first measurement, demonstrating that here, the local gate applied on Bob’s side immediately influences Alice’s measurement, violating the no-communication theorem.

The above protocol can be significantly generalized to an arbitrary number of fermionic modes, and involving any operator measured on Alice’s side  $O_A$ , and any gate  $U_B$  applied on Bob’s side, as long as both  $O_A$  and  $U_B$  are odd in fermion ladder operators. Note that while  $O_A, U_B$  being odd means that they change the fermion parity when being applied to a prepared state  $|\psi_A\rangle$ , they themselves do not violate the parity *superselection* rule: they change the parity of any state they are applied to, but they do not create superpositions of states with different parity. They do however always anticommute, such that we are guaranteed to find  $\langle \psi_A | U_B^\dagger O_A U_B | \psi_A \rangle = -\langle \psi_A | O_A | \psi_A \rangle$ . Hence, the only condition for this protocol to violate no-signalling is that  $\langle \psi_A | O_A | \psi_A \rangle \neq 0$ . Such a nonzero eigenvalue of an odd fermion operator can in turn only emerge if  $|\psi_A\rangle$  is in an even-odd superposition.

We now briefly outline, how this protocol is implemented. For this purpose, we consider the Majorana circuit (i.e., all Chern numbers equal 2) in the main text, with four nodes,  $Z = 4$ . We assign odd nodes 1 and 3 to Alice, and even nodes 2 and 4 to Bob. Choosing the same representation in terms of regular complex fermions as introduced in the main text, we identify  $a = c_1 = (\gamma_1 - i\gamma_3)/2$  and  $b = c_2 = (\gamma_2 - i\gamma_4)/2$ . The preparation of the vacuum state  $a|0\rangle = b|0\rangle = 0$  is outlined in Sec. 7 of the main text. The gate for the state initialization according to Eq. (52) is performed straightforwardly. We switch on a Josephson effect between ground and node 3 (on Alice’s side), yielding the Hamiltonian

$$H_A = -2\tilde{E}_J \gamma_3 = -2i\tilde{E}_J (a - a^\dagger). \quad (53)$$

Applying this Hamiltonian for time  $\tau = \pi/(8\tilde{E}_J)$  yields exactly the unitary time-evolution  $U_A$  as defined above. The measurement of  $O_A$  is realized by switching on a Josephson effect between ground and node 1, where the above introduced dispersive readout yields a projective measurement of  $O_A = \gamma_1 = a + a^\dagger$ . Bob can implement the gate  $U_B$  in two equivalent ways. Either, he switches on a Josephson effect between ground and node 2,

$$H_B = -2\tilde{E}_J\gamma_2 = -2\tilde{E}_J(b + b^\dagger), \quad (54)$$

this time, for double the time duration  $\tau = \pi/(4\tilde{E}_J)$ , or alternatively, he offsets the charge at node 2,  $n_2^{(\text{ext})}$ , by  $\pm 1$ . As demonstrated above, the expectation value measured on Alice's side swaps sign, depending on whether or not Bob performs gate  $U_B$ .

## References

- [1] L. Saminadayar, D. C. Glattli, Y. Jin and B. Etienne, *Observation of the  $e/3$  fractionally charged Laughlin quasiparticle*, Phys. Rev. Lett. **79**, 2526 (1997), doi:[10.1103/PhysRevLett.79.2526](https://doi.org/10.1103/PhysRevLett.79.2526).
- [2] R. de Picciotto, M. Reznikov, M. Heiblum, V. Umansky, G. Bunin and D. Mahalu, *Direct observation of a fractional charge*, Nature **389**, 162 EP (1997).
- [3] C. Castelnovo, R. Moessner and S. Sondhi, *Spin ice, fractionalization, and topological order*, Annual Review of Condensed Matter Physics **3**(Volume 3, 2012), 35 (2012), doi:<https://doi.org/10.1146/annurev-conmatphys-020911-125058>.
- [4] K. Flensberg, F. von Oppen and A. Stern, *Engineered platforms for topological superconductivity and Majorana zero modes*, Nature Reviews Materials **6**(10), 944 (2021), doi:[10.1038/s41578-021-00336-6](https://doi.org/10.1038/s41578-021-00336-6).
- [5] A. A. Odintsov and Y. V. Nazarov, *Incompressible quantum hall states in Josephson-junction arrays*, Phys. Rev. B **51**, 1133 (1995), doi:[10.1103/PhysRevB.51.1133](https://doi.org/10.1103/PhysRevB.51.1133).
- [6] R. Fazio and H. van der Zant, *Quantum phase transitions and vortex dynamics in superconducting networks*, Physics Reports **355**(4), 235 (2001), doi:[https://doi.org/10.1016/S0370-1573\(01\)00022-9](https://doi.org/10.1016/S0370-1573(01)00022-9).
- [7] F. Arute, K. Arya, R. Babbush, D. Bacon, J. C. Bardin, R. Barends, R. Biswas, S. Boixo, F. G. S. L. Brandao, D. A. Buell, B. Burkett, Y. Chen *et al.*, *Quantum supremacy using a programmable superconducting processor*, Nature **574**(7779), 505 (2019), doi:[10.1038/s41586-019-1666-5](https://doi.org/10.1038/s41586-019-1666-5).
- [8] A. Peres and D. R. Terno, *Quantum information and relativity theory*, Rev. Mod. Phys. **76**, 93 (2004), doi:[10.1103/RevModPhys.76.93](https://doi.org/10.1103/RevModPhys.76.93).
- [9] J. Bub, *Quantum mechanics is about quantum information*, Foundations of Physics **35**(4), 541 (2005), doi:[10.1007/s10701-004-2010-x](https://doi.org/10.1007/s10701-004-2010-x).
- [10] G. Chiribella, G. M. D'Ariano and P. Perinotti, *Informational derivation of quantum theory*, Phys. Rev. A **84**, 012311 (2011), doi:[10.1103/PhysRevA.84.012311](https://doi.org/10.1103/PhysRevA.84.012311).
- [11] N. Friis, *Reasonable fermionic quantum information theories require relativity*, New Journal of Physics **18**(3), 033014 (2016), doi:[10.1088/1367-2630/18/3/033014](https://doi.org/10.1088/1367-2630/18/3/033014).

- [12] N. Tibau Vidal, V. Vedral and C. Marletto, *A local-realistic theory for fermions*, AVS Quantum Science **4**(1), 013802 (2022), doi:[10.1116/5.0077220](https://doi.org/10.1116/5.0077220).
- [13] G. Viola and D. P. DiVincenzo, *Hall effect gyrators and circulators*, Phys. Rev. X **4**, 021019 (2014), doi:[10.1103/PhysRevX.4.021019](https://doi.org/10.1103/PhysRevX.4.021019).
- [14] R.-P. Riwar, M. Houzet, J. S. Meyer and Y. V. Nazarov, *Multi-terminal josephson junctions as topological matter*, Nature Communications **7**(1), 11167 (2016), doi:<https://doi.org/10.1038/ncomms11167>.
- [15] M. Rymarz, S. Bosco, A. Ciani and D. P. DiVincenzo, *Hardware-encoding grid states in a nonreciprocal superconducting circuit*, Phys. Rev. X **11**, 011032 (2021), doi:[10.1103/PhysRevX.11.011032](https://doi.org/10.1103/PhysRevX.11.011032).
- [16] A. Parra-Rodriguez, I. L. Egusquiza, D. P. DiVincenzo and E. Solano, *Canonical circuit quantization with linear nonreciprocal devices*, Phys. Rev. B **99**, 014514 (2019), doi:[10.1103/PhysRevB.99.014514](https://doi.org/10.1103/PhysRevB.99.014514).
- [17] B. Yurke and J. S. Denker, *Quantum network theory*, Phys. Rev. A **29**, 1419 (1984), doi:[10.1103/PhysRevA.29.1419](https://doi.org/10.1103/PhysRevA.29.1419).
- [18] D. Loss and K. Mullen, *Effect of dissipation on phase periodicity and the quantum dynamics of josephson junctions*, Phys. Rev. A **43**, 2129 (1991), doi:[10.1103/PhysRevA.43.2129](https://doi.org/10.1103/PhysRevA.43.2129).
- [19] C. Koliofoti and R.-P. Riwar, *Compact description of quantum phase slip junctions*, npj Quantum Information **9**(1), 125 (2023), doi:[10.1038/s41534-023-00790-w](https://doi.org/10.1038/s41534-023-00790-w).
- [20] K. Mullen, D. Loss and H. T. C. Stoof, *Resonant phenomena in compact and extended systems*, Phys. Rev. B **47**, 2689 (1993), doi:[10.1103/PhysRevB.47.2689](https://doi.org/10.1103/PhysRevB.47.2689).
- [21] E. Eriksson, R.-P. Riwar, M. Houzet, J. S. Meyer and Y. V. Nazarov, *Topological transconductance quantization in a four-terminal josephson junction*, Physical Review B **95**(7), 075417 (2017), doi:[10.1103/PhysRevB.95.075417](https://doi.org/10.1103/PhysRevB.95.075417).
- [22] J. S. Meyer and M. Houzet, *Nontrivial chern numbers in three-terminal josephson junctions*, Physical Review Letters **119**(13), 136807 (2017), doi:[10.1103/PhysRevLett.119.136807](https://doi.org/10.1103/PhysRevLett.119.136807).
- [23] V. Fatemi, A. R. Akhmerov and L. Bretheau, *Weyl josephson circuits*, Physical Review Research **3**(1), 013288 (2021), doi:[10.1103/PhysRevResearch.3.013288](https://doi.org/10.1103/PhysRevResearch.3.013288).
- [24] L. Peyruchat, J. Griesmar, J. D. Pillet and c. O. Girit, *Transconductance quantization in a topological josephson tunnel junction circuit*, Physical Review Research **3**(1), 013289 (2021), doi:[10.1103/PhysRevResearch.3.013289](https://doi.org/10.1103/PhysRevResearch.3.013289).
- [25] T. Herrig and R.-P. Riwar, *Cooper-pair transistor as a minimal topological quantum circuit*, Phys. Rev. Research **4**, 013038 (2022), doi:[10.1103/PhysRevResearch.4.013038](https://doi.org/10.1103/PhysRevResearch.4.013038).
- [26] R. L. Klees, J. C. Cuevas, W. Belzig and G. Rastelli, *Ground-state quantum geometry in superconductor-quantum dot chains*, Phys. Rev. B **103**, 014516 (2021), doi:[10.1103/PhysRevB.103.014516](https://doi.org/10.1103/PhysRevB.103.014516).
- [27] L. Teshler, H. Weisbrich, J. Sturm, R. L. Klees, G. Rastelli and W. Belzig, *Ground state topology of a four-terminal superconducting double quantum dot*, SciPost Phys. **15**, 214 (2023), doi:[10.21468/SciPostPhys.15.5.214](https://doi.org/10.21468/SciPostPhys.15.5.214).

- [28] H. Weisbrich, R. L. Klees, G. Rastelli and W. Belzig, *Second chern number and non-abelian berry phase in topological superconducting systems*, PRX Quantum **2**, 010310 (2021), doi:[10.1103/PRXQuantum.2.010310](https://doi.org/10.1103/PRXQuantum.2.010310).
- [29] E. Strambini, S. D'Ambrosio, F. Vischi, F. S. Bergeret, Y. V. Nazarov and F. Giazotto, *The  $\omega$ -squeezed as a tool to phase-engineer josephson topological materials*, Nature Nanotechnology **11**(12), 1055 (2016), doi:[10.1038/nnano.2016.157](https://doi.org/10.1038/nnano.2016.157).
- [30] N. Pankratova, H. Lee, R. Kuzmin, K. Wickramasinghe, W. Mayer, J. Yuan, M. G. Vavilov, J. Shabani and V. E. Manucharyan, *Multiterminal josephson effect*, Physical Review X **10**(3) (2020), doi:[10.1103/physrevx.10.031051](https://doi.org/10.1103/physrevx.10.031051).
- [31] M. Coraiola, D. Z. Haxell, D. Sabonis, H. Weisbrich, A. E. Svetogorov, M. Hinderling, S. C. ten Kate, E. Cheah, F. Krizek, R. Schott, W. Wegscheider, J. C. Cuevas *et al.*, *Phase-engineering the andreev band structure of a three-terminal josephson junction*, Nature Communications **14**(1), 6784 (2023), doi:[10.1038/s41467-023-42356-6](https://doi.org/10.1038/s41467-023-42356-6).
- [32] L. Peyruchat, R. H. Rodriguez, J.-L. Smirr, R. Leone and i. m. c. O. Girit, *Spectral signatures of nontrivial topology in a superconducting circuit*, Phys. Rev. X **14**, 041041 (2024), doi:[10.1103/PhysRevX.14.041041](https://doi.org/10.1103/PhysRevX.14.041041), [2401.10876](https://arxiv.org/abs/2401.10876).
- [33] R. P. Riwar, *Discrete control of capacitance in quantum circuits* (2023), [2306.00587](https://arxiv.org/abs/2306.00587).
- [34] F. Matute-Cañadas, L. Tosi and A. L. Yeyati, *Quantum circuits with multiterminal josephson-andreev junctions*, PRX Quantum **5**, 020340 (2024), doi:[10.1103/PRXQuantum.5.020340](https://doi.org/10.1103/PRXQuantum.5.020340).
- [35] P. Virtanen and T. T. Heikkilä, *Nonreciprocal josephson linear response*, Phys. Rev. Lett. **132**, 046002 (2024), doi:[10.1103/PhysRevLett.132.046002](https://doi.org/10.1103/PhysRevLett.132.046002).
- [36] D. Simms and N. Woodhouse, *Lectures on Geometric Quantization*, Lecture Notes in Physics. Springer Berlin Heidelberg, ISBN 9783540078609 (1976).
- [37] A. Cottet, *Implementation of a quantum bit in a superconducting circuit*, Ph.D. thesis, Université Paris VI (2002).
- [38] S. McArdle, S. Endo, A. Aspuru-Guzik, S. C. Benjamin and X. Yuan, *Quantum computational chemistry*, Rev. Mod. Phys. **92**, 015003 (2020), doi:[10.1103/RevModPhys.92.015003](https://doi.org/10.1103/RevModPhys.92.015003).
- [39] R. Barends, L. Lamata, J. Kelly, L. García-Álvarez, A. G. Fowler, A. Megrant, E. Jeffrey, T. C. White, D. Sank, J. Y. Mutus, B. Campbell, Y. Chen *et al.*, *Digital quantum simulation of fermionic models with a superconducting circuit*, Nature Communications **6**(1), 7654 (2015), doi:[10.1038/ncomms8654](https://doi.org/10.1038/ncomms8654).
- [40] U. E. Khodaeva, D. L. Kovrizhin and J. Knolle, *Quantum simulation of the one-dimensional fermi-hubbard model as a  $z_2$  lattice-gauge theory*, Phys. Rev. Res. **6**, 013032 (2024), doi:[10.1103/PhysRevResearch.6.013032](https://doi.org/10.1103/PhysRevResearch.6.013032).
- [41] S. Sachdev and J. Ye, *Gapless spin-fluid ground state in a random quantum heisenberg magnet*, Phys. Rev. Lett. **70**, 3339 (1993), doi:[10.1103/PhysRevLett.70.3339](https://doi.org/10.1103/PhysRevLett.70.3339).
- [42] A. Kitaev, *A simple model of quantum holography (part 1)*, <http://online.kitp.ucsb.edu/online/entangled15/kitaev/>, Talk at KITP, University of California, Santa Barbara, CA, U.S.A., 7 April 2015 (2015).

- [43] S. Lloyd, *Universal quantum simulators*, *Science* **273**(5278), 1073 (1996), doi:[10.1126/science.273.5278.1073](https://doi.org/10.1126/science.273.5278.1073).
- [44] D. Gottesman, A. Kitaev and J. Preskill, *Encoding a qubit in an oscillator*, *Phys. Rev. A* **64**, 012310 (2001), doi:[10.1103/PhysRevA.64.012310](https://doi.org/10.1103/PhysRevA.64.012310).
- [45] C. Berke, E. Varvelis, S. Trebst, A. Altland and D. P. DiVincenzo, *Transmon platform for quantum computing challenged by chaotic fluctuations*, *Nature Communications* **13**(1), 2495 (2022), doi:[10.1038/s41467-022-29940-y](https://doi.org/10.1038/s41467-022-29940-y).
- [46] E. Bocquillon, R. S. Deacon, J. Wiedenmann, P. Leubner, T. M. Klapwijk, C. Brüne, K. Ishibashi, H. Buhmann and L. W. Molenkamp, *Gapless andreev bound states in the quantum spin hall insulator hgte*, *Nature Nanotechnology* **12**(2), 137 (2017), doi:[10.1038/nnano.2016.159](https://doi.org/10.1038/nnano.2016.159).
- [47] G. C. Wick, A. S. Wightman and E. P. Wigner, *The intrinsic parity of elementary particles*, *Phys. Rev.* **88**, 101 (1952), doi:[10.1103/PhysRev.88.101](https://doi.org/10.1103/PhysRev.88.101).
- [48] A. Zee, *Quantum hall fluids*, In H. B. Geyer, ed., *Field Theory, Topology and Condensed Matter Physics*, pp. 99–153. Springer Berlin Heidelberg, Berlin, Heidelberg, ISBN 978-3-540-49455-3 (1995).
- [49] C. Bruder, R. Fazio and G. Schön, *The bose-hubbard model: from josephson junction arrays to optical lattices*, *Annalen der Physik* **517**(9-10), 566 (2005), doi:<https://doi.org/10.1002/andp.200551709-1005>, <https://onlinelibrary.wiley.com/doi/pdf/10.1002/andp.200551709-1005>.
- [50] D. Tong, *Lectures on the quantum hall effect* (2016), [1606.06687](https://arxiv.org/abs/1606.06687).
- [51] M. Cheng and N. Seiberg, *Lieb-Schultz-Mattis, Luttinger, and 't Hooft - anomaly matching in lattice systems*, *SciPost Phys.* **15**, 051 (2023), doi:[10.21468/SciPostPhys.15.2.051](https://doi.org/10.21468/SciPostPhys.15.2.051).
- [52] S. T. Chui and J. D. Weeks, *Phase transition in the two-dimensional coulomb gas, and the interfacial roughening transition*, *Phys. Rev. B* **14**, 4978 (1976), doi:[10.1103/PhysRevB.14.4978](https://doi.org/10.1103/PhysRevB.14.4978).
- [53] C. A. Mead and D. G. Truhlar, *On the determination of Born–Oppenheimer nuclear motion wave functions including complications due to conical intersections and identical nuclei*, *The Journal of Chemical Physics* **70**(5), 2284 (1979), doi:[10.1063/1.437734](https://doi.org/10.1063/1.437734).
- [54] R. L. Klees, J. C. Cuevas, W. Belzig and G. Rastelli, *Many-body quantum geometry in superconductor-quantum dot chains* (2020), [2009.11768](https://arxiv.org/abs/2009.11768).
- [55] E. Onofri, *Landau levels on a torus*, *International Journal of Theoretical Physics* **40**(2), 537 (2001), doi:[10.1023/A:1004115827959](https://doi.org/10.1023/A:1004115827959).
- [56] A. Metelmann and A. A. Clerk, *Nonreciprocal photon transmission and amplification via reservoir engineering*, *Phys. Rev. X* **5**, 021025 (2015), doi:[10.1103/PhysRevX.5.021025](https://doi.org/10.1103/PhysRevX.5.021025).
- [57] C. Leroux, A. Parra-Rodriguez, R. Shillito, A. D. Paolo, W. D. Oliver, C. M. Marcus, M. Kjaergaard, A. Gyenis and A. Blais, *Nonreciprocal devices based on voltage-tunable junctions* (2022), [2209.06194](https://arxiv.org/abs/2209.06194).
- [58] L.-A. Sellem, A. Sarlette, Z. Leghtas, M. Mirrahimi, P. Rouchon and P. Campagne-Ibarcq, *A gkp qubit protected by dissipation in a high-impedance superconducting circuit driven by a microwave frequency comb* (2023), [2304.01425](https://arxiv.org/abs/2304.01425).

- [59] F. D. M. Haldane and E. H. Rezayi, *Periodic Laughlin-Jastrow wave functions for the fractional quantized Hall effect*, Phys. Rev. B **31**, 2529 (1985), doi:[10.1103/PhysRevB.31.2529](https://doi.org/10.1103/PhysRevB.31.2529).
- [60] F. Gantmacher, *Theory of matrices*, Moscow: State Publishing House of technical and theoretical literature (1953).
- [61] N. Bourbaki, *Elements of mathematics, 2. Linear and multilinear algebra*, Addison-Wesley (1973).
- [62] W. Burnside, *Theory of groups of finite order*, Cambridge, The University Press (1897).
- [63] I. R. Charles W. Curtis, *Representation Theory of Finite Groups and Associative Algebras*, John Wiley & Sons, New York, London (1962).
- [64] W. Fulton and J. Harris, *Representation Theory: A First Course*, Graduate Texts in Mathematics. Springer New York, NY, 1 edn., doi:[10.1007/978-1-4612-0979-9](https://doi.org/10.1007/978-1-4612-0979-9) (1991).
- [65] W. J. Elion, J. J. Wachters, L. L. Sohn and J. E. Mooij, *Observation of the Aharonov-Casher effect for vortices in Josephson-junction arrays*, Phys. Rev. Lett. **71**, 2311 (1993), doi:[10.1103/PhysRevLett.71.2311](https://doi.org/10.1103/PhysRevLett.71.2311).
- [66] J. E. Mooij and Y. V. Nazarov, *Superconducting nanowires as quantum phase-slip junctions*, Nature Physics **2**(3), 169 (2006), doi:[10.1038/nphys234](https://doi.org/10.1038/nphys234).
- [67] I. M. Pop, B. Douçot, L. Ioffe, I. Protopopov, F. Lecocq, I. Matei, O. Buisson and W. Guichard, *Experimental demonstration of Aharonov-Casher interference in a Josephson junction circuit*, Phys. Rev. B **85**, 094503 (2012), doi:[10.1103/PhysRevB.85.094503](https://doi.org/10.1103/PhysRevB.85.094503).
- [68] O. V. Astafiev, L. B. Ioffe, S. Kafanov, Y. A. Pashkin, K. Y. Arutyunov, D. Shahar, O. Cohen and J. S. Tsai, *Coherent quantum phase slip*, Nature **484**(7394), 355 (2012), doi:[10.1038/nature10930](https://doi.org/10.1038/nature10930).
- [69] R. P. Riwar and D. P. DiVincenzo, *Circuit quantization with time-dependent magnetic fields for realistic geometries*, npj Quantum Information **8**(1), 36 (2022), doi:[10.1038/s41534-022-00539-x](https://doi.org/10.1038/s41534-022-00539-x).
- [70] K. Serniak, M. Hays, G. de Lange, S. Diamond, S. Shankar, L. D. Burkhardt, L. Frunzio, M. Houzet and M. H. Devoret, *Hot nonequilibrium quasiparticles in transmon qubits*, Physical Review Letters **121**(15), 157701 (2018), doi:[10.1103/PhysRevLett.121.157701](https://doi.org/10.1103/PhysRevLett.121.157701).
- [71] K. Serniak, S. Diamond, M. Hays, V. Fatemi, S. Shankar, L. Frunzio, R. J. Schoelkopf and M. H. Devoret, *Direct dispersive monitoring of charge parity in offset-charge-sensitive transmons*, Physical Review Applied **12**(1), 014052 (2019), doi:[10.1103/PhysRevApplied.12.014052](https://doi.org/10.1103/PhysRevApplied.12.014052).
- [72] D. Willsch, D. Rieger, P. Winkel, M. Willsch, C. Dickel, J. Krause, Y. Ando, R. Lescanne, Z. Leghtas, N. T. Bronn, P. Deb, O. Lanes *et al.*, *Observation of Josephson harmonics in tunnel junctions*, Nature Physics **20**(5), 815 (2024), doi:[10.1038/s41567-024-02400-8](https://doi.org/10.1038/s41567-024-02400-8).
- [73] S. M. Anton, J. S. Birenbaum, S. R. O’Kelley, V. Bolkhovsky, D. A. Braje, G. Fitch, M. Neeley, G. C. Hilton, H.-M. Cho, K. D. Irwin, F. C. Wellstood, W. D. Oliver *et al.*, *Magnetic flux noise in dc squids: Temperature and geometry dependence*, Phys. Rev. Lett. **110**, 147002 (2013), doi:[10.1103/PhysRevLett.110.147002](https://doi.org/10.1103/PhysRevLett.110.147002).

- [74] X. You, J. A. Sauls and J. Koch, *Circuit quantization in the presence of time-dependent external flux*, Phys. Rev. B **99**, 174512 (2019), doi:[10.1103/PhysRevB.99.174512](https://doi.org/10.1103/PhysRevB.99.174512).
- [75] R.-P. Riwar, *Charge quantization and detector resolution*, SciPost Physics **10**(4), 093 (2021), doi:[10.21468/scipostphys.10.4.093](https://doi.org/10.21468/scipostphys.10.4.093).
- [76] M. A. Rampp and J. Schmalian, *Integer and fractionalized vortex lattices and off-diagonal long-range order*, Journal of Physics Communications **6**(5), 055013 (2022), doi:[10.1088/2399-6528/ac7033](https://doi.org/10.1088/2399-6528/ac7033).
- [77] V. B. Geshkenbein, A. I. Larkin and A. Barone, *Vortices with half magnetic flux quanta in "heavy-fermion" superconductors*, Phys. Rev. B **36**, 235 (1987), doi:[10.1103/PhysRevB.36.235](https://doi.org/10.1103/PhysRevB.36.235).
- [78] H.-Y. Kee, Y. B. Kim and K. Maki, *Half-quantum vortex and d̄-soliton in sr<sub>2</sub>ruo<sub>4</sub>*, Phys. Rev. B **62**, R9275 (2000), doi:[10.1103/PhysRevB.62.R9275](https://doi.org/10.1103/PhysRevB.62.R9275).
- [79] D. A. Ivanov, *Non-abelian statistics of half-quantum vortices in p-wave superconductors*, Phys. Rev. Lett. **86**, 268 (2001), doi:[10.1103/PhysRevLett.86.268](https://doi.org/10.1103/PhysRevLett.86.268).
- [80] J. Ge, P. Wang, Y. Xing, Q. Yin, A. Wang, J. Shen, H. Lei, Z. Wang and J. Wang, *Charge-4e and charge-6e flux quantization and higher charge superconductivity in kagome superconductor ring devices*, Phys. Rev. X **14**, 021025 (2024), doi:[10.1103/PhysRevX.14.021025](https://doi.org/10.1103/PhysRevX.14.021025).
- [81] Y. Cao, J. Romero, J. P. Olson, M. Degroote, P. D. Johnson, M. Kieferová, I. D. Kivlichan, T. Menke, B. Peropadre, N. P. D. Sawaya, S. Sim, L. Veis *et al.*, *Quantum chemistry in the age of quantum computing*, Chemical Reviews **119**(19), 10856 (2019), doi:[10.1021/acs.chemrev.8b00803](https://doi.org/10.1021/acs.chemrev.8b00803).
- [82] M. P. Kaicher, S. B. Jäger, P.-L. Dallaire-Demers and F. K. Wilhelm, *Roadmap for quantum simulation of the fractional quantum hall effect*, Phys. Rev. A **102**, 022607 (2020), doi:[10.1103/PhysRevA.102.022607](https://doi.org/10.1103/PhysRevA.102.022607).
- [83] S. Sachdev and J. Ye, *Gapless spin-fluid ground state in a random quantum heisenberg magnet*, Physical review letters **70**(21), 3339 (1993).
- [84] Y. You and F. von Oppen, *Building fracton phases by majorana manipulation*, Phys. Rev. Res. **1**, 013011 (2019), doi:[10.1103/PhysRevResearch.1.013011](https://doi.org/10.1103/PhysRevResearch.1.013011).
- [85] M. Pretko, X. Chen and Y. You, *Fracton phases of matter*, International Journal of Modern Physics A **35**(06), 2030003 (2020), doi:[10.1142/S0217751X20300033](https://doi.org/10.1142/S0217751X20300033).
- [86] D. S. Abrams and S. Lloyd, *Quantum algorithm providing exponential speed increase for finding eigenvalues and eigenvectors*, Phys. Rev. Lett. **83**, 5162 (1999), doi:[10.1103/PhysRevLett.83.5162](https://doi.org/10.1103/PhysRevLett.83.5162).
- [87] M. Troyer and U.-J. Wiese, *Computational complexity and fundamental limitations to fermionic quantum monte carlo simulations*, Phys. Rev. Lett. **94**, 170201 (2005), doi:[10.1103/PhysRevLett.94.170201](https://doi.org/10.1103/PhysRevLett.94.170201).
- [88] J. B. James D. Whitfield and A. Aspuru-Guzik, *Simulation of electronic structure hamiltonians using quantum computers*, Molecular Physics **109**(5), 735 (2011), doi:[10.1080/00268976.2011.552441](https://doi.org/10.1080/00268976.2011.552441).
- [89] J. Preskill, *Quantum Computing in the NISQ era and beyond*, Quantum **2**, 79 (2018), doi:[10.22331/q-2018-08-06-79](https://doi.org/10.22331/q-2018-08-06-79).

- [90] S. B. Bravyi and A. Y. Kitaev, *Fermionic quantum computation*, Annals of Physics **298**(1), 210 (2002), doi:<https://doi.org/10.1006/aphy.2002.6254>.
- [91] V. c. v. Havlíček, M. Troyer and J. D. Whitfield, *Operator locality in the quantum simulation of fermionic models*, Phys. Rev. A **95**, 032332 (2017), doi:[10.1103/PhysRevA.95.032332](https://doi.org/10.1103/PhysRevA.95.032332).
- [92] M. Christandl, N. Datta, A. Ekert and A. J. Landahl, *Perfect state transfer in quantum spin networks*, Phys. Rev. Lett. **92**, 187902 (2004), doi:[10.1103/PhysRevLett.92.187902](https://doi.org/10.1103/PhysRevLett.92.187902).
- [93] M.-H. Yung, *Quantum speed limit for perfect state transfer in one dimension*, Phys. Rev. A **74**, 030303 (2006), doi:[10.1103/PhysRevA.74.030303](https://doi.org/10.1103/PhysRevA.74.030303).
- [94] L. Vinet and A. Zhedanov, *How to construct spin chains with perfect state transfer*, Phys. Rev. A **85**, 012323 (2012), doi:[10.1103/PhysRevA.85.012323](https://doi.org/10.1103/PhysRevA.85.012323).
- [95] R. J. Chapman, M. Santandrea, Z. Huang, G. Corrielli, A. Crespi, M.-H. Yung, R. Osellame and A. Peruzzo, *Experimental perfect state transfer of an entangled photonic qubit*, Nature Communications **7**(1), 11339 (2016), doi:[10.1038/ncomms11339](https://doi.org/10.1038/ncomms11339).
- [96] M. Nägele, C. Schweizer, F. Roy and S. Filipp, *Effective nonlocal parity-dependent couplings in qubit chains*, Phys. Rev. Res. **4**, 033166 (2022), doi:[10.1103/PhysRevResearch.4.033166](https://doi.org/10.1103/PhysRevResearch.4.033166).
- [97] D. Deutsch and P. Hayden, *Information flow in entangled quantum systems*, Proceedings of the Royal Society of London. Series A: Mathematical, Physical and Engineering Sciences **456**(1999), 1759 (2000), doi:[10.1098/rspa.2000.0585](https://doi.org/10.1098/rspa.2000.0585).
- [98] R. Clifton, J. Bub and H. Halvorson, *Characterizing quantum theory in terms of information-theoretic constraints*, Foundations of Physics **33**(11), 1561 (2003), doi:[10.1023/A:1026056716397](https://doi.org/10.1023/A:1026056716397).
- [99] P. Raymond-Robichaud, *A local-realistic model for quantum theory*, Proceedings of the Royal Society A: Mathematical, Physical and Engineering Sciences **477**(2250), 20200897 (2021), doi:[10.1098/rspa.2020.0897](https://doi.org/10.1098/rspa.2020.0897).
- [100] N. Friis, A. R. Lee and D. E. Bruschi, *Fermionic-mode entanglement in quantum information*, Phys. Rev. A **87**, 022338 (2013), doi:[10.1103/PhysRevA.87.022338](https://doi.org/10.1103/PhysRevA.87.022338).
- [101] M. Johansson, *Comment on 'reasonable fermionic quantum information theories require relativity'* (2016), [1610.00539](https://arxiv.org/abs/1610.00539).
- [102] P. Fendley, *Parafermionic edge zero modes in  $zn$ -invariant spin chains*, Journal of Statistical Mechanics: Theory and Experiment **2012**(11), P11020 (2012), doi:[10.1088/1742-5468/2012/11/P11020](https://doi.org/10.1088/1742-5468/2012/11/P11020).
- [103] D. P. Arovas, E. Berg, S. A. Kivelson and S. Raghu, *The hubbard model*, Annual Review of Condensed Matter Physics **13**(Volume 13, 2022), 239 (2022), doi:<https://doi.org/10.1146/annurev-conmatphys-031620-102024>.
- [104] U. Schollwöck, *The density-matrix renormalization group*, Rev. Mod. Phys. **77**, 259 (2005), doi:[10.1103/RevModPhys.77.259](https://doi.org/10.1103/RevModPhys.77.259).
- [105] J. Eisert, M. Cramer and M. B. Plenio, *Colloquium: Area laws for the entanglement entropy*, Rev. Mod. Phys. **82**, 277 (2010), doi:[10.1103/RevModPhys.82.277](https://doi.org/10.1103/RevModPhys.82.277).

- [106] F. Verstraete and J. I. Cirac, *Matrix product states represent ground states faithfully*, Phys. Rev. B **73**, 094423 (2006), doi:[10.1103/PhysRevB.73.094423](https://doi.org/10.1103/PhysRevB.73.094423).